POLITECNICO DI TORINO
Repository ISTITUZIONALE

Dynamic boronic ester cross-linkers enabling high-performance recyclable and room-temperature-curable epoxy vitrimers

Original
Dynamic boronic ester cross-linkers enabling high-performance recyclable and room-temperature-curable epoxy vitrimers / Sangaletti, D., Zych, A., Nardi, M., Fina, A., Perotto, G., Athanassiou, A.. - In: CELL REPORTS PHYSICAL SCIENCE. - ISSN 2666-3864. - STAMPA. - 7:5(2026), pp. 1-18. [10.1016/j.xcrp.2026.103262]

Availability:
This version is available at: 11583/3017226 since: 2026-10-30T09:19:03Z

Publisher:
Elsevier

Published
DOI:10.1016/j.xcrp.2026.103262

Terms of use:

This article is made available under terms and conditions as specified in the corresponding bibliographic description in the repository

Publisher copyright

(Article begins on next page)

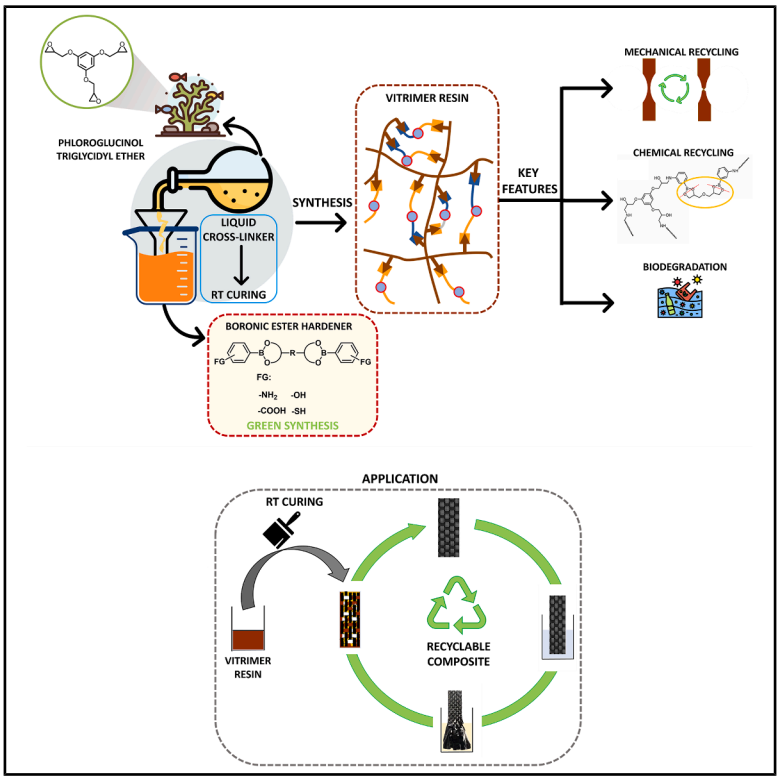
21 November 2026

Cell Reports
Physical Science

Article

Dynamic boronic ester cross-linkers enabling high-performance recyclable and room-temperature-curable epoxy vitrimers

Graphical abstract



Highlights

- Liquid boronic ester cross-linker enables epoxy vitrimer curing at RT
- High biobased epoxy vitrimer combines sustainability with mechanical performance
- Fully recyclable carbon-fiber composites enabled by vitrimer matrices

Authors

Davide Sangaletti, Arkadiusz Zych, Martina Nardi, Alberto Fina, Giovanni Perotto, Athanassia Athanassiou

Correspondence

davide.sangaletti@iit.it (D.S.), martina.nardi@iit.it (M.N.), giovanni.perotto@unipv.it (G.P.), athanassia.athanassiou@iit.it (A.A.)

In brief

Sangaletti et al. report on a liquid boronic ester cross-linker enabling room-temperature curing of epoxy vitrimers with significant biobased content. The resulting matrices deliver robust thermomechanical performance and enable fully recyclable carbon-fiber composites through dynamic covalent network exchange.

Sangaletti et al., 2026, Cell Reports Physical Science 7, 103262
May 20, 2026 © 2026 The Authors. Published by Elsevier Inc.
https://doi.org/10.1016/j.xcrp.2026.103262

CellPress

Cell Reports
Physical Science

CellPress
OPEN ACCESS

Article

Dynamic boronic ester cross-linkers enabling high-performance recyclable and room-temperature-curable epoxy vitrimers

Davide Sangaletti,[1,2,5,*] Arkadiusz Zych,[1] Martina Nardi,[1,*] Alberto Fina,[3] Giovanni Perotto,[1,4,*] and Athanassia Athanassiou[1,*]

[1]Smart Materials, Istituto Italiano di Tecnologia, Via Morego 30, 16163 Genova, Italy
[2]DIBRIS, University of Genoa, Viale Causa 13c, 16145 Genova, Italy
[3]Department of Applied Science and Technology, Politecnico di Torino, Viale Teresa Michel 5, 15121 Alessandria, Italy
[4]Present address: Department of Chemistry, University of Pavia, Viale Torquato Taramelli 10, 27100 Pavia, Italy
[5]Lead contact
*Correspondence: davide.sangaletti@iit.it (D.S.), martina.nardi@iit.it (M.N.), giovanni.perotto@unipv.it (G.P.), athanassia.athanassiou@iit.it (A.A.)
https://doi.org/10.1016/j.xcrp.2026.103262

SUMMARY

Epoxy thermosets are widely used in industry, for example, in carbon-fiber coatings, because of their strong mechanical performance and chemical resistance. However, their permanently cross-linked structure prevents recycling, causing environmental accumulation. Epoxy-based vitrimers offer a potential solution by incorporating dynamic covalent bonds into their 3D networks, allowing reprocessing, similar to thermoplastics, while retaining thermoset stability. To match the simple preparation of conventional epoxies, boronic ester vitrimers require liquid, easily miscible cross-linkers that cure epoxy precursors at room temperature without solvents. This study synthesized nine new boronic ester cross-linkers containing amino, carboxylic acid, hydroxy, or thiol groups and evaluated their thermal behavior, stability, and curing efficiency. The best candidate enabled vitrimer formation through a ring-opening click reaction, curing at room temperature and post-curing at 60°C. The resulting materials showed strong mechanical properties, shape memory, recyclability, improved seawater biodegradation, and suitability for recyclable high-performance fiber-reinforced composites.

INTRODUCTION

Vitrimers are a class of polymers comprising a dynamic covalent bonding network that combines the characteristics of thermosets and thermoplastics.[1] Thermally activated exchangeable bonds cause a rearrangement of their 3D structure, allowing self-healing properties and reprocessability typical of thermoplastics.[2] In contrast, vitrimers result in a stable covalent structure, similar to thermosetting polymers, when temperatures are below the proper activation temperature, demonstrating mechanical strength and resistance. First introduced in 2011 by Liebler and coworkers,[3] interest in vitrimers has been continuously growing, leading to the production of 198 papers only in 2022.[4] Over the years, several vitrimer structures have been proposed, exploiting dynamic bonding exchange through, for instance, *trans*-esterification bonds,[5,6] disulfide exchange,[7] imine metathesis,[8] boronic ester exchange,[9,10,11,12] and siloxane exchange.[13,14] The activation of the exchange reactions follows Arrhenius's law, where the activation energy (E_a) indicates the minimum energy required to promote the dynamic reactions. The Arrhenius E_a of the majority of the above-mentioned exchange reactions ranges between 7 and 170 kJ mol^{-1}, depending on the catalyst added and the network's chemical structure.[2] Vitrimers with relatively high E_a demonstrate network stability but require higher temperatures for reprocessing, which can potentially damage the chemical network integrity while being energy consuming. Among vitrimer dynamic reactions, boronic ester exchange is certainly of interest, since it allows rapid network rearrangements without additional catalysts and under relatively mild conditions. In fact, boronic-ester-based vitrimers present Arrhenius E_a in the range of 7.7–142 kJ mol^{-1},[15–21] the lowest range among the other dynamic systems described above, enabling lower reprocessing temperatures and shorter times.[9,10,17] Vitrimers bearing boronic ester moieties in their structure are prepared either by the reaction of boronic acid with alcohol pendant groups[21,22] or by mimicking the general epoxy resins' thermosetting preparation, where an epoxy precursor and a hardener are mixed together to generate the network structure via the epoxy ring-opening reaction.[9,12] From a technological point of view, creating vitrimers using the epoxy resins' curing mechanism has several advantages. Two of the main ones are the possible use of thermosetting epoxy precursors already on the market and the absence of by-product formation during the curing based on the nucleophile-epoxy opening click mechanism.

This is an open access article under the CC BY-NC-ND license (http://creativecommons.org/licenses/by-nc-nd/4.0/).

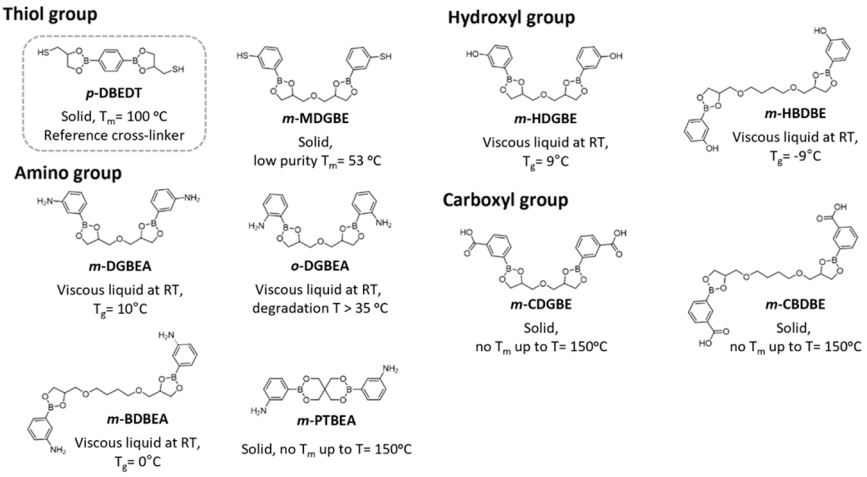


Figure 1. Structures of the prepared boronic ester cross-linkers

Structures of the boronic ester cross-linkers prepared in this work grouped by functional group and their thermal characterization (T_m, melting temperature; T_g, glass transition temperature; T, temperature). p-DBEDT was synthetized according to a procedure previously published.[10]

In commercially available epoxy resins, both epoxy-functionalized pre-polymer and polyamine hardener cross-linkers are viscous liquids that can be easily mixed at room temperature (RT) and subsequently heat cured. Vitrimer cross-linkers containing boronic esters are still far from the polyamine hardeners in terms of easy handling and application. They are typically solid at RT and not soluble in many epoxy molecules, which prevents convenient mixing at RT in the absence of solvents. Indeed, one of the factors that limit the replacement of epoxy thermosets with their boronic vitrimer counterparts is the scarce number of easy-to-use liquid cross-linkers and the high energy required for the curing process.[9,12] These limitations can be overcome by introducing novel boronic ester cross-linkers in liquid form that can be easily miscible with common epoxy precursors and that can be used in place of amino hardeners for the production of recyclable thermosets. Addressing these shortcomings is thus of fundamental importance to exploit the boronic ester vitrimers in many applications that require lower curing temperatures and easy preparation.

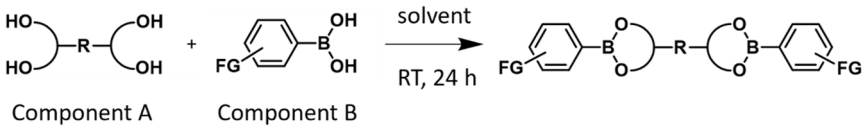
In this work, we aim to fill this gap by synthesizing nine novel aromatic boronic-ester-functionalized molecules in order to obtain liquid boronic ester cross-linkers that can be easily mixed with common epoxy building blocks and cured at temperatures ranging from RT to about 120°C. The thermal properties together with their curing efficiency in the epoxy ring-opening reaction have also been investigated to identify the most promising cross-linkers. Boronic ester cross-linkers were prepared by permutation of two blocks:

- component A (the core of the cross-linker), which consists of alkyl compounds with diol functionalization at both ends, selected from diglycerol, pentaerythritol, and hydrolyzed 1,4-butanediol diglycidyl ether (BDGE), and
- component B (the reactive tails of the cross-linker), which consists of boronic acid benzenes substituted with either carboxylic acid or hydroxyl or amine or thiol groups (Figure 1; Scheme 1; Table S1).

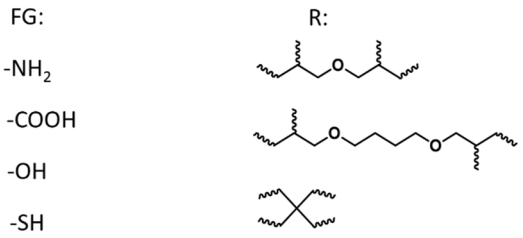
Apart from the choice of the cross-linker, the selection of epoxy building block precursors is equally important. Many epoxy precursors, such as bisphenol A diglycidyl ether, derive from petroleum, are not biodegradable, and are potentially harmful to the environment and to human health.[23] Recently, examples of biobased precursor building blocks were employed in vitrimer and thermoset preparation.[24,25] Examples are plant oils,[9,10,26,27] isosorbide,[28–30] lignin derivatives,[31,32] and the brown algae derivative phloroglucinol triglycidyl ether (PHTE).[33–35] The last is of special interest, since its use can decrease the reliance on petroleum-derived feedstocks owing to its high biobased carbon content, thus contributing to development of more sustainable materials in line with the United Nations' Sustainable Development Goal 17 (SDG17).[36]

One of main applications for which the vitrimers are considered a good substitution for thermoset resins is high-performance fiber-reinforced polymer composites (FRPCs).[37] FRPCs comprise a polymer matrix and high-strength fibers. They are largely used in automotive, structural, aerospace, and submarine applications.[38] Global FRPC production reached 13 million tons in 2023, with an increasing projected growth of the market at a compound annual growth rate (CAGR) of 7.84% from €210 billion in 2021 to €357 billion by 2028.[39,40,41] Conventional FRPCs have no practical end of life, due to the impossibility of recycling or reprocessing. Vitrimers are proposed as a sustainable matrix alternative for high-performance FRPCs because the possibility of their reprocessing can provide an option for their end of life.[42–44] Our group has recently proposed a vegetable-oil-based vitrimer matrix for FRCPs able to be fully chemically recyclable and biodegradable in seawater, while it gives similar mechanical and thermal properties compared with FRCPs made from commercial epoxy thermosets.[9] In that work, boronic ester exchangeable bonds were incorporated into the vitrimer network by reaction of a thiol-functionalized boronic ester cross-linker and epoxidized linseed oil at 140°C for 15 h. Even if the recycling efficiency and the mechanical properties of the vegetable-oil-based vitrimers were outstanding and apparently offered a good alternative to commercial epoxy resins in FRCP applications, the temperature and time required for vitrimer synthesis still pose important limitations for a convenient substitution of epoxy thermoset.

For this reason, our purpose of finding a suitable boronic ester cross-linker able to cure epoxy precursors at temperatures between RT and 60°C represents a strong improvement in the use of boronic ester vitrimers in FRCP applications. Nine molecules with variable cores and different functional groups for the epoxy curing reaction have been synthetized. Four of them



Scheme 1. General scheme of the cross-linker synthesis



were liquid at RT and easily miscible with common epoxy resin pre-polymers. Among these, the best cross-linker structure turned out to have a diglycerol core, which we showed provided the highest gel fraction (GF), and two amino groups in the meta position relative to the boronic moiety, which allow for lowest curing temperature. The cross-linker, named *m*-DGBEA, was able to react with epoxy pre-polymers (EPPs) at RT, completing the curing within 24 h, making this material the first boronic vitrimer curable under ambient conditions. With a post-curing treatment of 3 h at 60°C, a GF up to 99% could be obtained.

Using *m*-DGBEA as the cross-linker, vitrimers were synthesized with a commercial EPP or with a high biobased-content building block: PHTE. The bending test on the vitrimers showed a brittle behavior similar to that of a commercial epoxy resin. Moreover, thanks to the dynamic nature of the materials, stress relaxation, thermomechanical reshaping, and a shape memory effect were demonstrated.

The vitrimers displayed two options for recycling: thermomechanical, employing compression molding at 100°C, and chemical recycling under mild conditions in aqueous ethanol solution followed by solvent casting. Both the cross-linker and the vitrimers exhibited improved biodegradation behavior under marine conditions compared with a conventional epoxy thermoset. Although complete biodegradation was not achieved within the test period, the enhanced degradation suggests a reduced risk of long-term accumulation in marine environments.

Finally, in order to demonstrate the feasibility of replacing epoxy thermosets in real applications, the developed PHTE-based vitrimers were used as a matrix for the preparation of high-performance FRPCs. The vitrimer-based composites exhibited mechanical performance and density very similar to those of traditional composites made with commercial epoxy resin, and we also demonstrated how they can be fully recycled by recovering both the vitrimer matrix and the reinforcement carbon-fiber layers.

While this study demonstrates a significant advancement in the development of RT-curable and liquid boronic ester cross-linkers, offering a route to a viable end of life for high-performance composites, several limitations remain to be addressed in future research. A primary consideration is the hydrolytic stability of the boronic ester linkage. Although we took advantage of its susceptibility to hydrolysis to enable efficient chemical recycling in aqueous ethanol, the long-term durability of these vitrimers in high-humidity environments, or during prolonged immersion in water, requires further investigation.

Second, although the PHTE-based vitrimer exhibited measurable biodegradation in seawater, complete mineralization was not achieved within the experimental time frame. Understanding the degradation kinetics and the fate of the degradation products is essential for a comprehensive environmental impact assessment. In this context, a dedicated life-cycle assessment (LCA) study would be highly valuable to quantitatively evaluate the overall environmental footprint of these materials.

Additionally, while the biobased content reached 45% in this study, future efforts should aim for 100% biobased formulations by exploring alternative renewable epoxy precursors and optimizing the synthesis of cross-linkers from fully sustainable feedstocks.

From an industrial perspective, the 24-h curing time at RT, while energy efficient, may still represent a bottleneck for high-throughput manufacturing processes. Future studies could investigate new reactions or catalysts to accelerate curing without compromising the vitrimer behavior. Finally, while we successfully produced and recycled carbon fiber composites at a laboratory scale, testing these materials in larger structural components will be a crucial step toward their practical adoption in the automotive and aerospace sectors, which are the most prominent industries for the application of high-performance composite materials.

RESULTS AND DISCUSSION

Design of novel boronic ester cross-linkers

The general scheme of the cross-linker synthesis is reported in Scheme 1, and the final cross-linker structures are shown in Figure 1. For comparison, we synthesized the *p*-DBEDT cross-linker (Figure S4) employed in a previous work of our group.[10] Component A, the core of the cross-linker, was selected from three different molecules with two-diol functionalization. Of these three molecules, diglycerol and pentaerythritol are commercially available, while a diol with a longer chain was obtained from the hydrolysis of BDGE (it is commonly used in combination with bisphenol A in the synthesis of epoxy resins).

It is worth noting that, when diglycerol was employed as component A, the presence of impurities such as glycerol (3%) and polyglycerols (28%) (Figure S1) led to a small amount of boronic cross-linkers with varying core lengths. Furthermore, ^{1}H NMR analysis indicated that the final mixtures contained small amounts of unreacted reagents, with conversion rates for

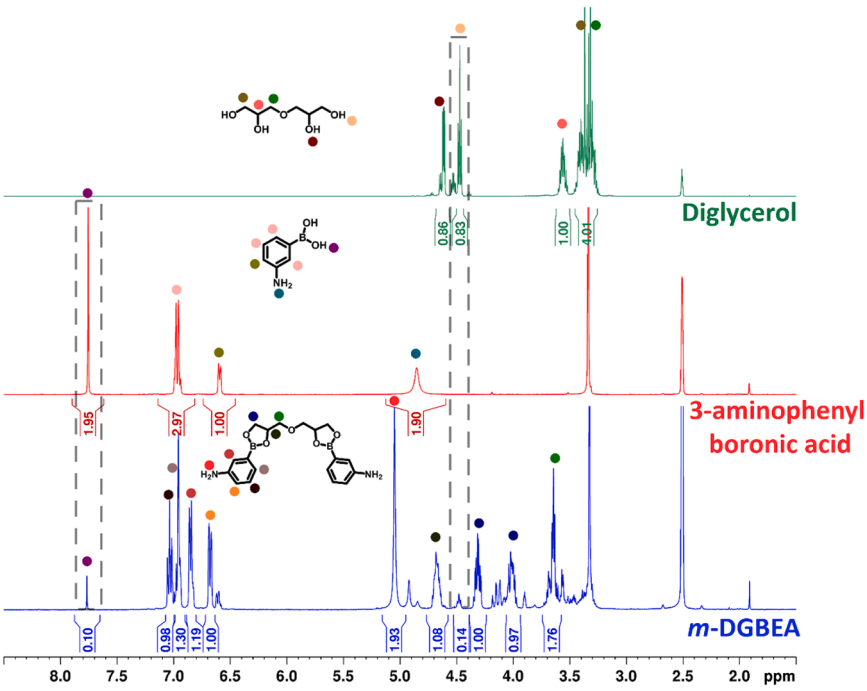


Figure 2. ^{1}H NMR spectra for the determination of the *m*-DGBEA formation

^{1}H NMR of diglycerol, 3-aminophenylboronic acid, and the resulting *m*-DGBEA in DMSO-d_6.

the target products typically ranging between 90% and 95%. Despite the presence of these species, further purification of the final cross-linkers was not performed after solvent removal. This approach was adopted to evaluate the efficiency of the "as-synthesized" products in epoxy curing and to prioritize a simplified, cost-effective protocol suitable for potential industrial scale-up. Notably, the presence of these minor impurities and by-products did not prejudice the formation of the vitrimer network. This is supported by the high GFs achieved (95% for the EPP-vitrimer and 99% for the PHTE-vitrimer) and the excellent mechanical, thermal, and recycling properties of the resulting materials, which remained comparable to those expected from high-purity systems. These results suggest that the robust nature of the material after the curing process allows for high-performance vitrimer even without rigorous purification of the cross-linking agents.

After 24 h the product of the reaction between component A and component B was analyzed by ^{1}H NMR analysis. The results for all the synthesized cross-linkers are reported in Figures S5, S6, S7, S8, S9, S10, S11, S12, and S13, while in Figure 2, the ^{1}H NMR spectrum of the *m*-DGBEA is shown as a characteristic example. Peaks at 7.9 ppm of the hydroxy groups of 3-aminophenyl boronic acid and peaks at 4.2–4.4 ppm associated with the OH groups of diglycerol simultaneously disappeared, while new peaks appeared in the aromatic and alkyl region associated with the formation of the target boronic ester cross-linker *m*-DGBEA. It is worth noting that, in the final mixture, 10% unreacted 3-aminophenyl boronic acid is still present, indicating that *m*-DGBEA has been obtained with a yield of 90%. In addition to the ^{1}H NMR spectrum, *m*-DGBEA has been further characterized with ^{13}C NMR and 2D NMR measurements as shown in Figure S7. In addition to the chemical characterization, thermogravimetric analysis (TGA) and differential scanning calorimetry (DSC) analysis were performed to establish the thermal stability and potential temperature transitions (Figure S7). To further demonstrate the strength and versatility of the cross-linker preparation, we carried out *m*-DGBEA synthesis in other additional green solvents, such as acetone, ethyl acetate (EtOAc), methyl tetrahydrofuran (Me-THF), and anisole (Figure S3). The possibility of ranging among several organic media offers a great advantage, since a significant intent of green chemistry is to decrease the use of solvents or use less toxic ones. In fact, concerns about the effects of many solvents on human health and the environment are increasing.[45]

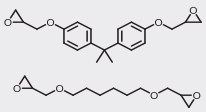
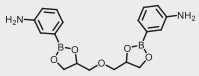
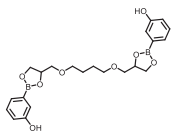
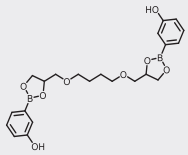
For the synthesis of other cross-linkers, ethanol was chosen as the solvent, since it allows the solubilization of the reagents in a few minutes. The reaction was successful for most of the target products and the final cross-linkers were characterized by means of ^{1}H NMR and ^{13}C NMR, while the thermal properties were assessed via TGA and DSC analysis (Figures S5, S6, S7, S8, S9, S10, S11, S12, and S13).

As our results show (Figure 2), cross-linkers with a diglycerol core were generally obtained as a viscous liquid, except for the product derived from boronic acid benzene with carboxylic acid functionalization, which resulted in a solid at RT with no T_m up to 150°C. Among the liquid cross-linkers, *o*-DGBEA showed degradation at temperature just above 35°C (Figure S6) and could not be employed for vitrimer synthesis.

Cross-linkers with a longer alkyl chain in the core encompass a lower glass transition temperature (T_g) (Figure S8), as shown from the comparison between the molecules prepared starting from the hydrolyzed BDGE and those prepared from diglycerol (Figure S7). Characteristic examples include cross-linkers derived from 3-aminophenyl boronic acid or 3-hydroxybenzene boronic acid. Replacing the core with a more hindered structure, such as pentaerythritol, resulted in a solid cross-linker, with no T_m up to 120°C. For example, 3-aminophenyl boronic acid produced viscous liquid cross-linkers with either diglycerol or hydrolyzed BDBEA (butanediol diboronic ester diamino) (*m*-DGBEA and *m*-BDBEA). In contrast, it produced a solid cross-linker with a pentaerythritol core (*m*-PTBEA [*meta*-pentaerythritol diboronic ester diamino]). This result is similar to that of a cross-linker used in previous works (*p*-DBEDT), which had an aromatic core and a T_m of 100°C. Generally, T_g is a key parameter of polymers, with the Flory-Fox equation correlating the T_g to their molecular weight. The original model is valid for

CellPress
OPEN ACCESS

Table 1. Composition, curing conditions, and gel fractions of vitrimers with the novel liquid cross-linkers

Vitrimer name	Component A (epoxy compound) (g)	Component B (cross-linker) (g)	Curing temperature (°C)	Gel fraction (curing) (%)	Gel fraction (post-curing) (%)
Sample A1	 EPP, 5.51	 *m*-DGBEA, 6.49	RT, post-curing at 60°C	80	95
Sample A2	EPP, 4.98	 *m*-BEBEA, 7.02	RT, post-curing at 60°C	48	66
Sample H1	EPP, 5.50	 *m*-HDGBE, 6.50	120	87	–
Sample H2	EPP, 4.97	*m*-HBDBE, 7.03	120	66	–

molecular weight higher than 1,000 Da,[46,47] which does not comprise the range of molecular weights of the synthetized cross-linkers in this work (range from 466 to 494 Da). However, studies on supercooled liquids and small molecules having a rubbery to glass transition have found that small molecules such as lactic acid (M_W = 90.08 g/mol) or sugar can show a T_g.[48]

Lactic acid and sugar have a different molecular structure compared with our cross-linkers, and they are capable of strong hydrogen bonding interactions between molecules. As a consequence, T_g is visible in the supercooled state at 0.6–0.8 T_m. Our cross-linkers have a structure comprising a flexible alkyl core and two aromatic functionalized tails. The functional groups in the aromatic ring are able to form hydrogen bonds, while the aromatic rings give rise to π-π interactions. Similar to lactic acid and sugar molecules, we may ascribe the presence of a glass to rubbery transition in some of synthetized cross-linkers to the presence of non-covalent interactions, such as hydrogen bonding.

In conclusion, looking at the structures of the different synthesized cross-linkers, it can be stated that the structure of the tetraol significantly affects the T_m and the T_g. In general, flexible liquid tetraols such as diglycerol and hydrolyzed BDGE allow one to obtain liquid products, in contrast to pentaerythritol. In long linear molecular chains or structures, the individual molecules are more flexible and have greater freedom of movement, and this mobility often interferes with the ability of molecules to arrange themselves into an ordered, crystalline structure. Instead, these molecules might favor an amorphous or less ordered arrangement.[45] The kind of reactive functional groups in the phenyl ring of the boronic acid also plays an important role. In fact, cross-linkers with amino and hydroxy groups were liquid, while the molecules containing carboxylic acid groups were solid, probably due to the strong hydrogen bonding between carboxylic acid groups compared with amino or hydroxyl groups. A similar trend is also visible by looking at the T_m of butanediamine (T_m = 27.5°C), butanediol (T_m = 20.1°C), and butane dicarboxylic acid or adipic acid (T_m = 152.1°C).[45–48] Finally, the position of the functional group in the aromatic ring of the final cross-linker has a negligible influence on the T_m, while it plays an important role in the thermal stability of the product.

In summary, only *m*-DGBEA, *m*-BDBEA, *m*-HDGBE (dihydroxyl diglycerol diboronic ester), and *m*-HBDBE (dihydroxyl butanediol diboronic ester) were obtained as viscous liquids at RT (Table 1) and were therefore tested in epoxy-based vitrimer curing.

Efficiency of novel liquid cross-linker with conventional EPP

The curing efficiency of the four selected liquid cross-linkers was tested by a reaction with one of the most used commercially available EPPs, composed of a mixture of bisphenol A diglycidyl ether and BDGE, and we compared the GF and the reaction rate of the prepared vitrimers. The samples' names and results are shown in Table 1.

The vitrimers prepared with amino-functionalized cross-linkers (samples A1 and A2) required lower curing temperature (24 h at RT + 3 h at 60°C) compared with the cross-linkers bearing hydroxyl groups (samples H1 and H2, which required 120°C). This can be explained by the higher reactivity of amines, which are better nucleophiles, toward epoxy groups. The GF of the resulting vitrimers reflects the degree of cross-linking in the materials. GF was higher for the cross-linkers characterized by a shorter alkyl chain: samples A1 and H1 showed higher GF,

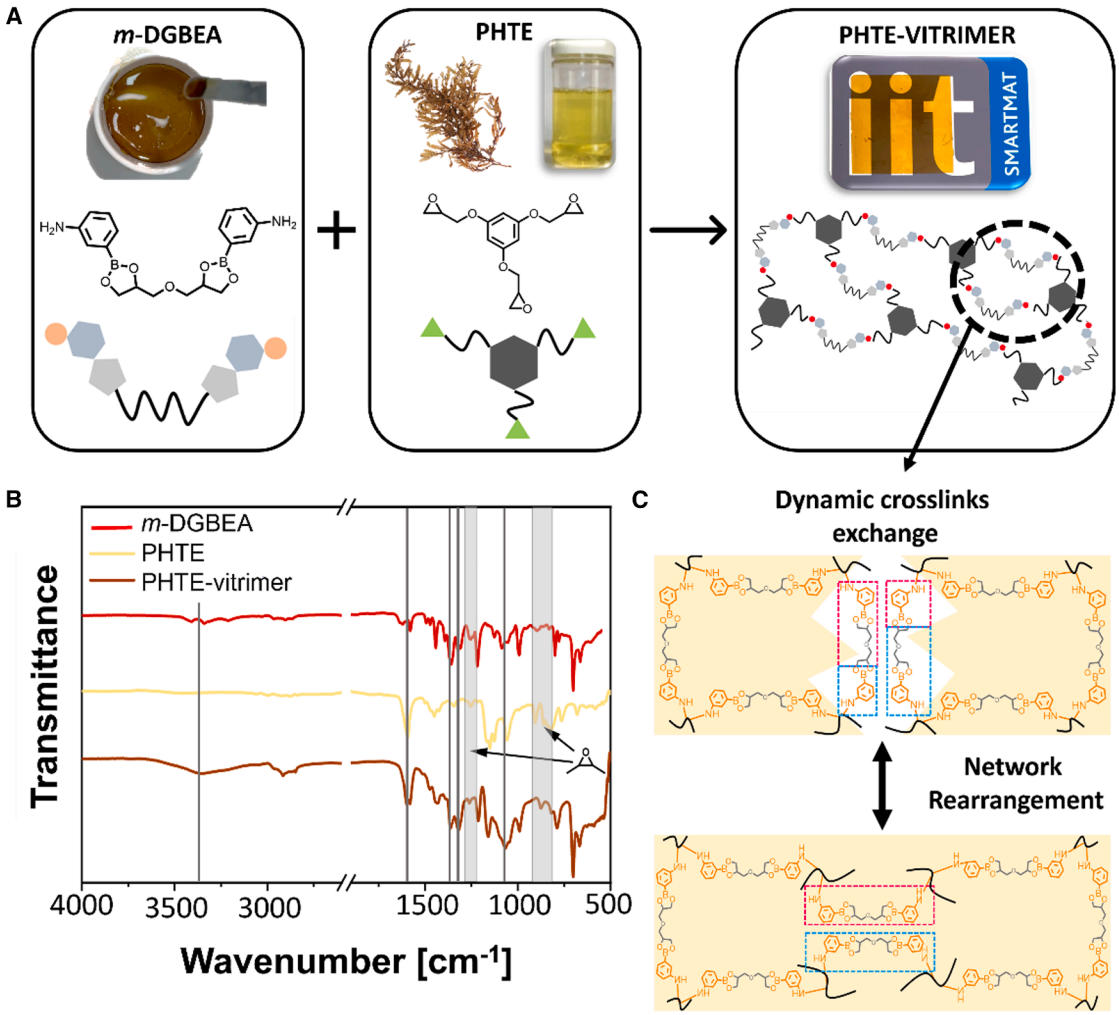


Figure 3. Synthesis of the PHTE-vitrimer

(A) Schematic representation of the PHTE-vitrimer synthesis.

(B) Infrared (IR) spectrum of the PHTE-vitrimer synthesis.

(C) Scheme of the network rearrangement by boronic ester exchange.

90% and 86%, respectively, compared with A2 and H2, which had GF of 66%.

In summary, *m*-DGBEA gave the best curing results, since it was able to synthesize vitrimers at RT, with a post-curing of 3 h at 60°C and a GF higher than 90%, similar to commercial epoxy thermosets. Because of this, *m*-DGBEA was selected for the synthesis of vitrimers with two different building blocks: the high-biobased-content PHTE and the commercial EPP.

Fabrication and characterization of vitrimers with high biobased content

In an effort to replace fossil building blocks used in the synthesis of plastics with renewable ones, PHTE was chosen because it is partially derived from brown algae (biobased carbon content of 60% as specified by the supplier)[33] and is characterized by three epoxy groups per molecule that can participate in the cross-linking reaction with the boronic ester diamine cross-linker (we confirmed the structure using ^{1}H NMR, as shown in Figure S14). *m*-DGBEA and PHTE were cured by simply mixing them at RT, at an epoxy-to-amine ratio of 1 (Figure 3A), taking advantage of the liquid state of both components, without the need for any solvent. The curing leverages the amino-epoxy click reaction, and after 24 h at RT a transparent, slightly orange and rigid material was obtained, as shown in Figure 3 and Table S2. The material underwent a post-curing process at 60°C for 3 h to increase the GF, as described in the previous paragraph. Overall, the final biobased content of the PHTE-based vitrimer is 45%, meaning that nearly half of its mass is derived from renewable resources, as shown by calculation in Scheme S1.

Similarly, a vitrimer composed by *m*-DGBEA and EPP and a standard epoxy thermoset derived by curing EPP with a commercial amine hardener have been used as reference materials. Reaction efficiency, thermal and mechanical properties, and recycling performance of the vitrimer materials were thus

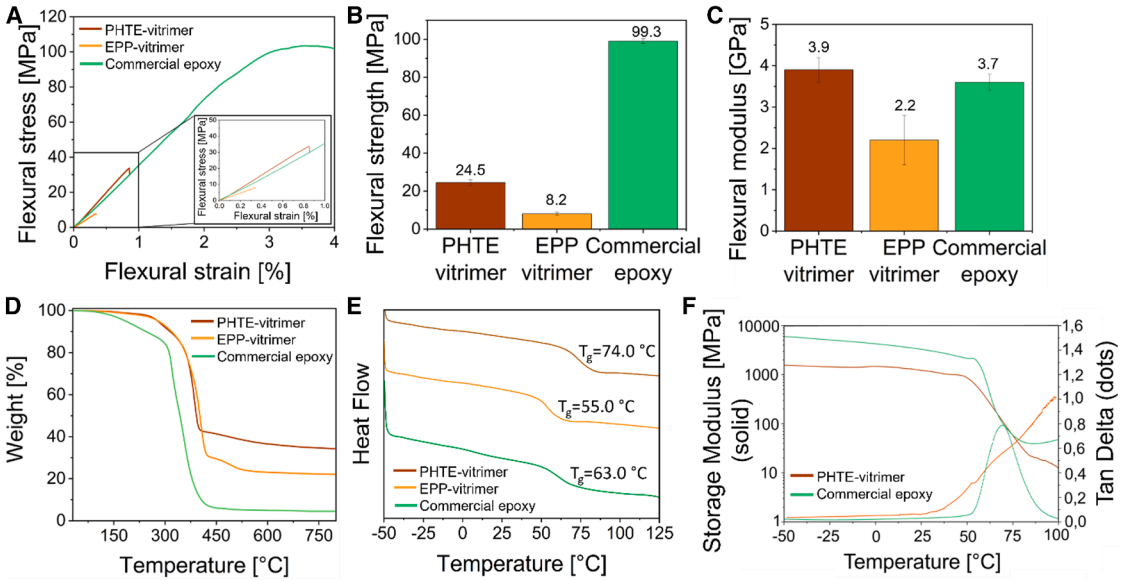


Figure 4. Mechanical properties of the vitrimers and commercial epoxy

Typical flexural curve (A), flexural modulus (B), and flexural strength (C) of PHTE- and EPP-vitrimers and commercial epoxy; TGA (D) and DSC (E) curves of vitrimers and commercial epoxy; and DMTA curves of PHTE-vitrimer and commercial resin (F). Data are represented as the mean ± SD.

compared with a standard epoxy thermoset (Figures S15 and S16; Table S2).

The GF in EtOAc of the two vitrimers and the thermoset was evaluated over time, and the results are shown in Figure S17. EtOAc was chosen because it is a good solvent for all the boronic ester cross-linkers and epoxy precursors (DGBEA pre-polymer and PHTE) but not for the final vitrimers. The PHTE-vitrimer reached a GF of 88% after 20 h, and post-curing allowed the GF to increase by up to 99%. EPP-vitrimer shows a GF of 80% after 24 h at RT, which could reach 95% after post-curing. The commercial epoxy thermoset was able to achieve a GF of 99% after 24 h curing at RT. In addition, the resistance of the vitrimer with higher biobased content (PHTE-vitrimer) was tested in several additional solvents, including acetone, 2-propanol, anisole, and chloroform. The results showed that the material maintained its visual characteristics (shape and color) and showed no weight loss after 24 h immersion, indicating an excellent solvent resistance (Figure S18; Table S4).

The cross-linking reactions were monitored using Fourier transform infrared (FTIR) spectrometry, as shown in Figure 3C. In the PHTE-vitrimer spectrum, the disappearance of the epoxy-related bands (1,252 cm^{-1}, assigned to the symmetric ring breathing; 906 cm^{-1}, attributed to the asymmetric stretching of the C–O–C epoxy ring; and 861 cm^{-1}, corresponding to its symmetric stretching) is accompanied by the appearance of new peaks at 1,599 cm^{-1} (aromatic C=C stretching), 1,579 cm^{-1} (N–H bending), 1,067 cm^{-1} (C–O–C stretching), and a broad band at 3,360 cm^{-1} (N–H stretching), which are consistent with the reaction between the epoxy groups and the amine functionalities of *m*-DGBEA. Similarly, in the EPP-vitrimer (Figure S19), the epoxy-related peaks at 1,247, 909, and 860 cm^{-1} disappear, while new bands at 1,580 cm^{-1} (aromatic C=C stretching), 1,610 cm^{-1} (aromatic C=C stretching), and 3,343–3,409 cm^{-1} (N–H stretching) appear, further confirming the successful cross-linking and vitrimer network formation.

These results confirmed that *m*-DGBEA is a good cross-linker, because high GF could be achieved with a commercial epoxy base (EPP) and a building block with high biobased content (PHTE) with similar cross-linking kinetics. We hypothesize that the small difference in kinetic and final GF might be due to the presence of dynamic boronic ester bonds that could slowly rearrange during the curing.

Thermomechanical properties of vitrimers

The mechanical properties of the different materials were characterized statically with a bending test and dynamically by dynamic mechanical thermal analysis (DMTA). For stress-deformation tests, only flexural modulus was characterized, since specimens were slipping out of the clamps.[9] The typical bending test curves are reported in Figure 4A, and the results are summarized in Figures 4B and 4C. PHTE-vitrimer showed an average flexural modulus of 3.9 GPa and flexural strength around 29 MPa, while the EPP-vitrimer showed an average flexural modulus of 2.2 GPa and low flexural strength around 8 MPa, making it very fragile. Instead, the epoxy resin showed an average flexural modulus of 3.6 GPa and flexural strength of 99 MPa. It is important to highlight that no significant differences in mechanical properties were observed in the two vitrimers, or in the epoxy thermoset, before or after post-curing, as reported in Figure S20.

The DMTA test, reported in Figure 4F, shows that the storage modulus of the PHTE-vitrimer remains nearly constant in the temperature range between −50°C and 60°C due to its stable cross-link density, exhibiting a behavior very similar to that of the conventional thermoset. However, as the temperature approaches 90°C, the storage modulus of the PHTE-vitrimer

begins to gradually decrease because of the dynamic nature of its covalent network, which allows stress relaxation and molecular rearrangement (Figure S21).

The relaxation curves shown in Figure S22A clearly highlight the different behaviors between the PHTE-vitrimer and the thermoset: while the thermoset maintains a nearly constant stress over time when the sample is deformed, indicating a permanent covalent network that does not allow any relaxation of the stress, the PHTE-vitrimer exhibits a rapid decrease in the load required to stretch the material, and this relaxation becomes more pronounced at higher temperatures. This is the signature behavior of the dynamic network of the vitrimer: the exchange reactions between the boronic esters allow for molecular rearrangement and relaxation of the stress. Tests with the EPP-vitrimer were not possible due to its brittleness.

Two important parameters are used to describe the dynamic network of vitrimers: the activation energy (E_a) of the bond exchange and the topological freezing temperature (T_v) of the material.

The E_a can be determined from the crossover point of the frequency sweep, according to a previously described method.[10,49,50] From the frequency sweeps shown in Figure S22B, the PHTE-vitrimer exhibits a solid-like behavior up to 80°C, characterized by a fairly constant storage modulus (G′) that is higher than the loss modulus (G″). At higher temperatures, G″ becomes higher than G′, indicating a transition to a viscoelastic liquid-like regime, as expected due to the activation of boronic ester exchange reactions, which enable flow and processability (Figure 3C).

The crossover point moves toward shorter timescales (higher frequency) with increasing temperature, which means that the material relaxes stress and flows faster, as previously mentioned. The crossover frequency can be used to determine the E_a,[10] which for the PHTE-vitrimer was calculated to be 90 kJ/mol. This value is higher than the typical E_a reported for boronic ester vitrimers, which usually ranges between 7.7 and 13.8 kJ/mol up to 38.9 kJ/mol.[19–21] E_a is influenced by several parameters, including the chemistry of the exchange reaction (boronic esters in this work), the rigidity of the building blocks used, and the presence of catalysts or plasticizers. In our system the aromatic ring at the core of PHTE is much more rigid than the building blocks reported in the literature, causing the observed increase in E_a. Similarly, higher values for E_a were observed in cyclic compounds, where values between 76.7 and 142 kJ/mol were measured.[15–18]

The second important parameter that characterizes vitrimers is the topology freezing transition temperature of vitrimers, T_v. Below T_v, the reaction rate of exchange is almost negligible, while above T_v the exchange rate is high enough to produce an effect. For the PHTE-vitrimer, the calculated T_v was 10°C. This temperature indicates that boronic ester exchange is thermally accessible even at mild temperatures, although the rearrangements of the boronic ester bonds are limited by chain mobility. T_v values for other boronic ester-vitrimer systems vary from temperatures well below 0°C up to 90°C, depending on the network chemistry and cross-linker flexibility. For example, in our previous works, the T_v of the boronic ester vitrimers prepared from vegetable oils ranged between −121°C and ≈ −55°C.[9,10] Zhao et al. synthesized a methylvinyl silicone vitrimer encompassing boronic ester bonds that exhibited a T_v of ≈6°C, while other bio-based vitrimers prepared starting from tannic acid, glycerol, and boric acid have T_v values of 40°C.[15,21,51,52]

Finally, DSC was used to measure the T_g of the different materials (results are summarized in Figure 4E). The PHTE-vitrimer showed a T_g of 74°C, higher than that of the epoxy thermoset, which had a T_g of 63°C, and that of the EPP-vitrimer, which showed a T_g of 58°C. This can most likely be attributed to the higher content of aromatic rings coming from both the phloroglucinol and the boronic ester diamine cross-linker.

For the PHTE-vitrimer, the T_v (10°C) is significantly lower than the T_g (74°C). This means that even though the exchange reactions could occur, below the T_g they are prevented due to restricted chain mobility. When the material is heated just above the T_g, segmental motion is slowly initiated, while the exchange reactions have already plenty of thermal energy to happen very quickly, resulting in the fast stress relaxation previously observed. With further increase in the temperature, the boronic ester exchange dominates the network rearrangements, reflected in a viscosity decrease even lower, following Arrhenius's law,[10,53,54] as is clearly shown in Figures S22B and S22C.

Rheological analysis of the EPP-vitrimer reveals a behavior similar to that of the PHTE-vitrimer. Below 60°C the material behaves as a solid, exhibiting a relatively constant storage modulus (G′) that is significantly higher than the loss modulus (G″). Above 60°C the boronic ester exchange accelerates, allowing the material to flow and be processed. However, compared to the PHTE-vitrimer, the crossover point shifts to shorter timescales (higher frequencies) as the temperature increases, indicating a much faster stress relaxation and flow behavior. Moreover, since the crossover point moves beyond the measurable range above 100°C, the relaxation kinetics become extremely fast, preventing an accurate determination of the E_ay (Figure S23).

TGA was used to understand the thermal stability of the different materials. Results, reported in Figure 4D, show that the both the PHTE-vitrimer and the EPP-vitrimer were stable and did not decompose for temperatures up to around 250°C, while the commercial epoxy starts to lose weight at 150°C, probably due to the evaporation of some additives present inside the resin.

Furthermore, the PHTE-vitrimer has a density around 1.23 g/cm^3, the EPP-vitrimer around 1.34 g/cm^3, and the commercial epoxy around 1.13 g/cm^3 (Table S5). The higher density observed in the vitrimer systems compared with the epoxy resin suggests a more efficient molecular packing and/or a higher cross-linking density. This characteristic can be advantageous, as it is typically associated with enhanced mechanical strength and improved dimensional stability. However, higher density leads also to higher material weight, which is less desirable in lightweight structural applications. The obtained density values fall into the typical density range of epoxy resins (≈1.1–1.4 g/cm^3).

The peculiar thermomechanical properties of vitrimers and their capability to release stress over time can be used to reshape materials but also to provide shape memory effects. When reshaping is performed at low temperature (100°C) and for only 60 s, a new shape ("C" shape) can be obtained, but the vitrimer retains the residual stress. The new shape is maintained once the sample is cooled, but because the stress is

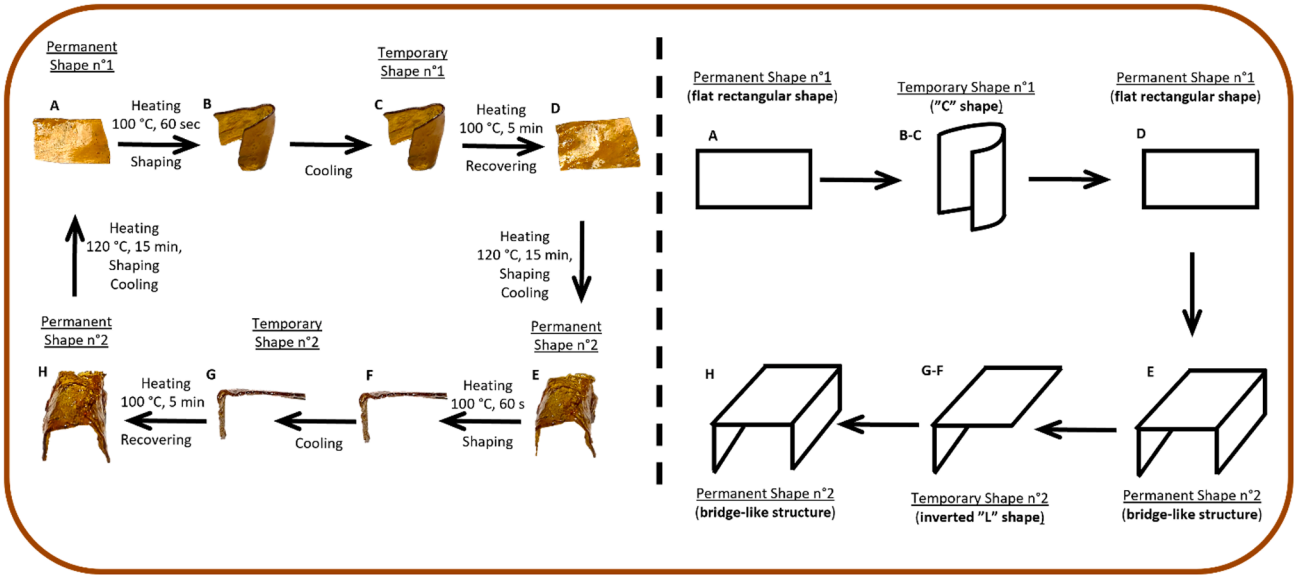


Figure 5. Shape reconfiguration of the PHTE-vitrimer

Shape memory effect and permanent shape transformation of the PHTE-vitrimer.

retained in the material, the original shape (flat rectangular shape) can be restored by reheating at 100°C for 5 min, as shown in Figures 5A–5D. Since this process is reversible, it enables shape-memory materials with multiple shape transformations.[55] Vitrimers, though, can also undergo permanent shape changes when sufficient heat and time are provided. For instance, as shown in Figures 5D and 5E, by heating at 120°C for 15 min, the samples can be reshaped from a flat 2D rectangular geometry into a 3D bridge-like structure. Subsequently, the shape can be further modified into a temporary inverted "L" configuration (Figures 5E–5G), which is fixed upon cooling. Later, the original geometry can be fully recovered by heating the vitrimer again at 100°C for 5 min, as shown in in Figures 5G and 5H.

Unlike vitrimers, conventional epoxy thermosets can be temporarily reshaped but lack the ability to release stress and achieve permanent transformations due to their static cross-linked network, as shown in Figure S24.

Vitrimer recycling

Recycling highly cross-linked materials, such as thermosets, presents significant challenges due to their thermal, mechanical, and chemical stability, properties essential for their widespread success. However, the dynamic cross-linking of vitrimers offers a solution to this challenge. Boronic ester vitrimers, such as the ones studied here, enable two potential recycling pathways: thermal-mechanical reprocessing via dynamic bond exchange reactions and chemical reprocessing through the reversible hydrolysis of the boronic ester bonds.

Mechanical recycling of PHTE- and EPP-vitrimer is shown in Figures 6A and 6B, respectively. The materials were ground into powder and subsequently compression-molded at 100°C for 5 min under 3 tons of pressure, creating a new transparent and uniform recycled material. Grinding and hot pressing were repeated up to four times, without significant changes in the flexural modulus (Figures 6D–6I and Figure S25), cross-link density (Tables S6 and S7), or chemical structure (Figures S26 and S27).

For example, the bending modulus of the reprocessed vitrimers remained indistinguishable from that of the virgin materials: approximately 3.9 GPa for the PHTE-vitrimer and 2.2 GPa for the EPP-vitrimer. Thermal analysis confirmed that the recycled vitrimers maintained thermal stability up to about 250°C, like the materials before recycling. Finally, the GF of the reprocessed materials was comparable to that of the pristine ones, confirming the stability and robustness of the developed high-biobased-content boronic ester vitrimers. In contrast, the commercial epoxy thermoset could not be reprocessed under the same conditions, and when it was compression-molded, it merely fragmented into small pieces that failed to fuse together under the tested conditions (Figure 6C), consistent with observations reported in the previous paper.[9]

Boronic ester bonds allowed for good resistance to different organic solvents, such as THF, isopropanol, and acetone, similar to the epoxy thermoset. One of their unique features is the possibility for the boronic ester bonds to be hydrolyzed[56,57] with a 90:10 v/v solution of ethanol and water, as shown in Figures 7A and 7B. Once dissolved, these bonds can be reformed after solvent evaporation, re-creating the dynamically cross-linked network and offering a pathway for an effective chemical recycling route for these materials.

For chemical recycling, the dissolution of the vitrimers (1 g of PHTE vitrimer in 15 mL of a water-ethanol mixture) could occur at RT, although the process is very slow. However, heating the mixture to 60°C resulted in vitrimer dissolution within 20 min, resulting in a homogeneous solution, as reported in Figures 7A and 7B. FTIR spectrometry and TGA of the chemically recycled film shown in Figures S26 and S27 confirmed that it was possible to fully recover the original solid material by a simple casting of the solution.

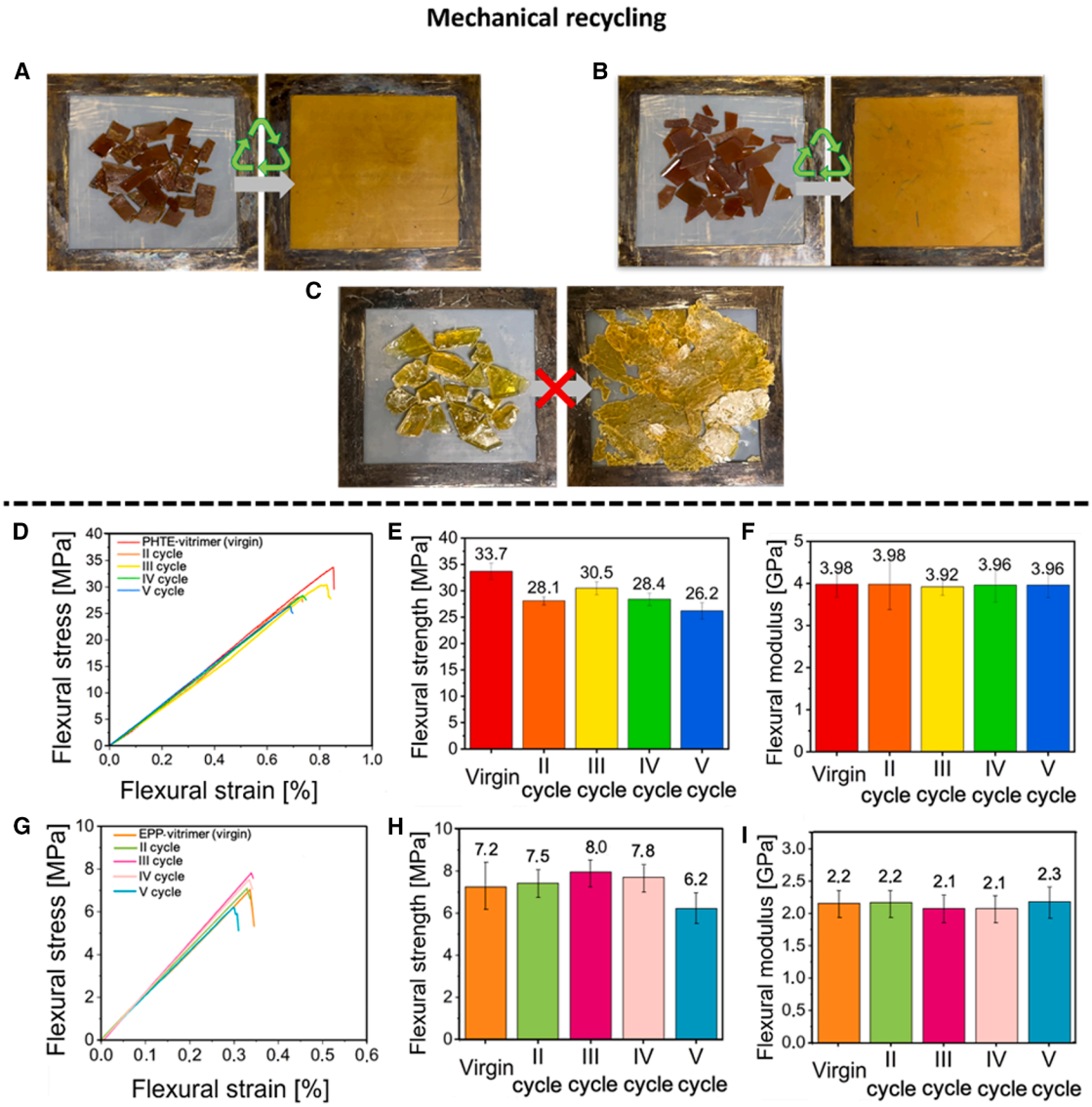


Figure 6. Mechanical recycling of the vitrimers

(A–C) Mechanically recycled PHTE-vitrimer (A) and EPP-vitrimer (B) and comparison with commercial epoxy (C) under 3 tons of pressure for 5 min at 100°C. (D–I) Typical bending curve (D), flexural strength (E), and flexural modulus (F) of the virgin (cycle I) and the reprocessed (cycles II–V) PHTE-vitrimer, and bending curve (G), flexural strength (H), and flexural modulus (I) of the virgin and the reprocessed EPP-vitrimer (the error bars shown in all the graphs indicate the standard deviation of the measurements). Data are represented as the mean ± SD.

To confirm that the hydrolysis of the boronic ester bonds was responsible for the dissolution of the PHTE-vitrimer, ^{1}H NMR analysis of the dissolved vitrimer was acquired in aqueous deuterated dimethyl sulfoxide (DMSO-d_6). The resulting spectrum showed the presence of the boronic acid -OH groups and those of the free diglycerol (Figure S28) as a result of the boronic ester hydrolysis. Similar to PHTE-vitrimer, ^{1}H NMR of hydrolyzed EPP-vitrimer (Figure S29) confirmed the hydrolysis of boronic ester bonds.

As is well known, the commercial epoxy thermoset cannot be chemically recycled under the same conditions (Figure 7C).

The recycling was much more efficient in comparison to previous work conducted by our group,[9] since it required lower temperature and shorter time to complete the hydrolysis. We hypothesize that the difference might be mainly due to the lower cross-linking density of the PHTE-vitrimer compared with the previous vitrimer material (3 epoxy groups per PHTE molecule versus 5.6 epoxy groups per epoxidized linseed oil).

Biodegradability

The biodegradability in seawater of the two prepared vitrimers was determined by biochemical oxygen demand (BOD) and compared with that of the commercial epoxy thermoset, polypropylene, and cotton (Figure 7D).

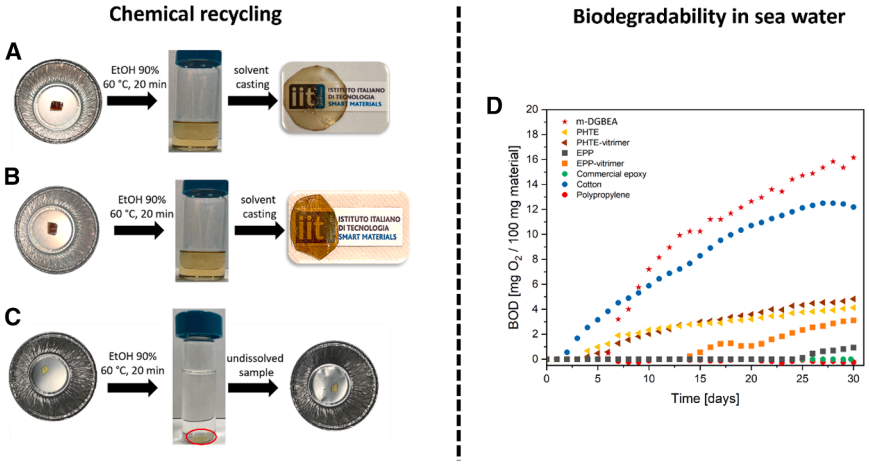


Figure 7. Chemical recycling of the vitrimers and BOD

Chemical recycling of the vitrimers by hydrolysis and dissolution in 90% v/v ethanol at 60°C for 20 min and subsequent solvent casting to regenerate the vitrimer as a thin, transparent film (A and B), and comparison with commercial epoxy (C); BOD of the PHTE-vitrimer, EPP-vitrimer, and their precursors and commercial epoxy, cotton fabric, and polypropylene as reference (D).

PHTE-vitrimer starts to biodegrade after only 4 days in seawater. We hypothesize that the fast onset of the biodegradation is due to the hydrolysis of boronic ester linkages. Within a month the BOD reached values of 5 mg O_2/100 mg material. Instead, the EPP-vitrimer starts to biodegrade after 15 days, reaching the value of 3.1 mg O_2/100 mg material, indicating a lower biodegradability rate. The cotton fabric (in blue) reached 12.5 mg O_2/100 mg material, while the polypropylene (in red) and the commercial epoxy remained close to 0 mg O_2/100 mg for the entire time (Figure 7D).

It should be noted that the BOD value does not directly correspond to the fraction of material mineralized but rather reflects the oxygen consumption associated with microbial activity during the degradation of organic matter. According to ISO 14851, the degree of biodegradation should ideally be expressed as a percentage relative to theoretical oxygen demand (ThOD). The ThODs of *m*-DGBEA ($C_{18}H_{22}B_2N_2O_5$) and PHTE ($C_{15}H_{18}O_6$) were therefore calculated based on their elemental composition, yielding a value of 170 mg O_2 per 100 mg of material for *m*-DGBEA and 180 mg O_2 per 100 mg for PHTE. On this basis, biodegradation percentages of 9.5% for *m*-DGBEA and 2.4% for PHTE were obtained. In addition, the ThOD and the biodegradation degree were also calculated for the PHTE-vitrimer, considering a repeating unit formed by PHTE and *m*-DGBEA in a 1:2 molar ratio, giving a ThOD value of 210 mg O_2 per 100 mg of material and a biodegradation percentage of 2.5%. For comparison, the same approach was applied to the cotton fabric used as a reference (cellulose repeating unit), resulting in a ThOD of 102.6 mg O_2 per 100 mg and a biodegradation degree of 12.2%.

We hypothesize that the rapid onset of oxygen consumption is primarily driven by the hydrolysis of boronic ester linkages, which enhances network accessibility to microbial activity. This interpretation is supported by the fast biodegradation of the *m*-DGBEA cross-linker, which exhibited a higher oxygen consumption rate than cellulose under the same conditions. Consistently, both vitrimers showed higher oxygen consumption than the commercial epoxy reference, with the PHTE-vitrimer displaying the fastest onset and the highest BOD. This behavior is in line with its higher biobased content and increased hydrolytic susceptibility. The measured BOD values are comparable to those reported for other boronic-ester-based systems (2–11 mg O_2/100 mg),[9,10] further supporting the biodegradation potential of these materials. Although the overall extent of biodegradation remains limited compared with natural materials such as cotton, the rapid initial oxygen uptake observed for the PHTE-vitrimer suggests enhanced hydrolytic sensitivity, which may confer environmental safety advantages over conventional, non-degradable thermosets in the event of accidental release.

FRPCs based on vitrimers

The possibility of chemically recycling the vitrimers synthesized here could be exploited in the preparation of FRPCs using PHTE-vitrimer as a matrix. The easy chemical recycling of the vitrimer would allow the separation, purification, regeneration, and reuse of both the matrix and the reinforcements, a process that is not possible for traditional epoxy resin thermosets.

To demonstrate this, two composites with three carbon-fiber layers using the new high-biobased-content PHTE-vitrimer and the EPP-vitrimer were prepared by hand layup and compared with an epoxy thermoset composite. Details of the preparation are described in the Methods. The PHTE-vitrimer-based composite showed an average elastic modulus of 25 GPa and a flexure strength of 396 MPa, values that are very similar to those of the commercial epoxy composite (elastic modulus of 23 GPa and a flexural strength of 290 MPa) (Figures 8F, 8G, and 8H), while the EPP-vitrimer-based composite showed a flexural modulus of 20 GPa and lower flexural strength (160 MPa), showing a more fragile behavior, similar to what was shown previously in this work. In general, the composites exhibited comparable flexural stiffness; in particular, the flexural moduli were very similar for all systems, since the carbon fibers bear the greatest part of the load. However, marked differences were observed in flexural strength, with the PHTE-based composite being distinctly stronger than the EPP-based one. The one-way ANOVA based on the flexural modulus confirmed a statistically significant difference between the two vitrimer-based composites, as was also reflected in their flexural strength. However, no statistically significant difference was found between the flexural moduli of the vitrimer and the epoxy composites, indicating insufficient statistical evidence to conclude that they exhibit distinct properties (Figure S30).

Moreover, to evaluate the quality of the vitrimer composites in terms of impregnation capability of the resin, SEM and optical

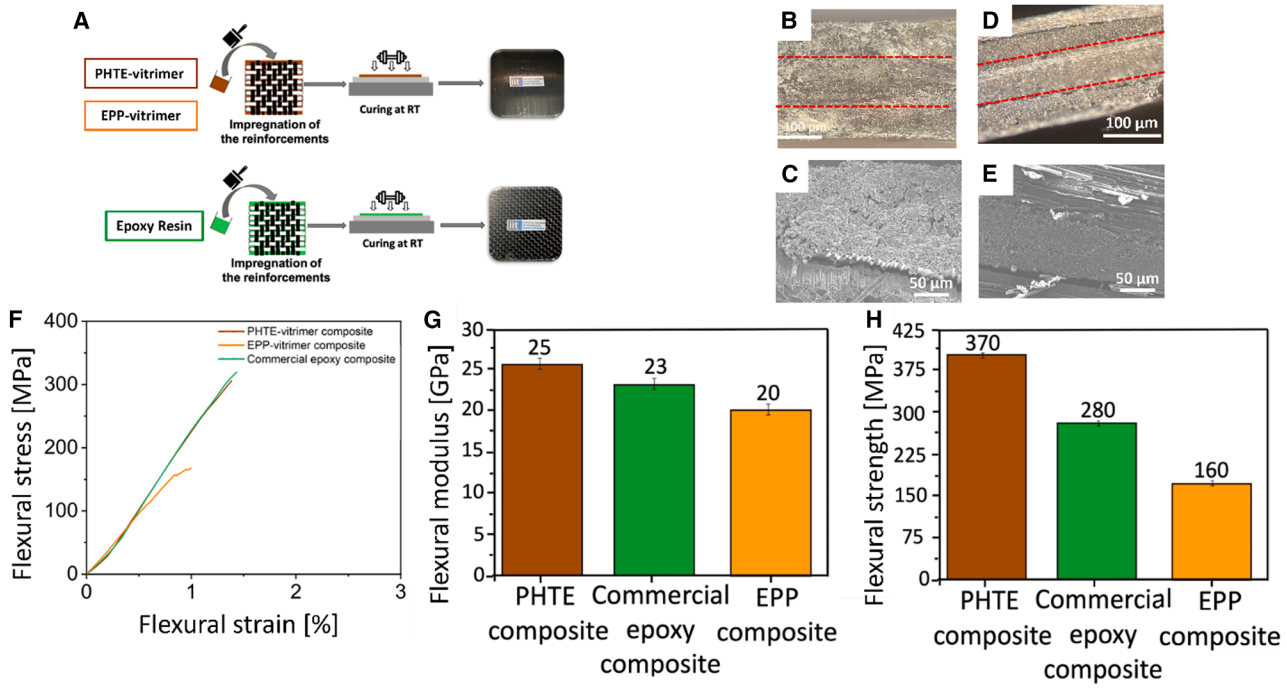


Figure 8. Mechanical properties of the composites

(A) Fabrication of the carbon-fiber-reinforced composites.

(B–E) Optical microscope images of a cross section of the PHTE-vitrimer composite (B) and commercial epoxy composite (D); SEM images of a cross section of the PHTE-vitrimer composite (C) and the commercial epoxy composite (E).

(F–H) Typical flexural curve (F), flexural strength (G), and flexural modulus (H) of the vitrimer composites and the commercial epoxy composite (the error bars shown in all the graphs indicate the standard deviation of the measurements). Data are represented as the mean ± SD.

microscopy were employed. Images of a cross section of the PHTE-vitrimer (Figure 8B) revealed an excellent interfacial bonding between the carbon fibers and the matrices (Figure 8C). Indeed, both vitrimers, as well as the commercial epoxy thermoset (Figures 8D and 8E), impregnated the carbon fibers very well, ensuring a good adhesion between the layers without exfoliation or slippage between the carbon layers, and that is reflected in the high flexural strength for all three composites. The TGA showed that, for the commercial epoxy composite, the percentage of the matrix was (epoxy resin) 48.3% w/w and the reinforcement (carbon fibers) 51.7% w/w (Figure S31; Scheme S2). On the other hand, for the PHTE-vitrimer composites the percentage was 47.6% w/w reinforcements and 52.4% w/w matrix, and for the EPP-vitrimer composites it was 48.7% w/w reinforcements and 51.3% w/w matrix (Table S8). The densities of both composites were very similar, since the densities of both the matrices (vitrimer and commercial epoxy) were quite close (Table S5).

To take advantage of the chemical recycling abilities of the two vitrimers synthesized here, vitrimer-based FRCPs were treated with 90% v/v ethanol solution at 60°C for 3 h (Figures 9A and S32). Thanks to the hydrolysis of the boronic ester linkages of the PHTE-vitrimer resin, it was possible to recover both the vitrimer matrix and the carbon fibers from the composite under very mild conditions.

At the end of the process, the three carbon-fiber layers could be easily separated, washed with fresh EtOH 90% v/v, and dried under ambient conditions. The vitrimer itself could be regenerated as well by simple evaporation of the solvent. By employing the chemical recycling, more than 99% of the carbon fibers and vitrimer matrix were recovered (Table S8).

After the recovery of the carbon fibers, surface morphology and mechanical properties were further determined by optical microscopy, SEM, X-ray diffraction (XRD), and Raman spectroscopy. The SEM analysis showed that the morphology of the recovered carbon fibers was indistinguishable from that of the pristine fibers, proving the effectiveness of the recycling process. In addition, from the optical microscopy and SEM analysis, it was notable that the recycled carbon fibers did not have any vitrimer residues attached (Figures 9B and 9C).

Furthermore, the XRD and Raman spectroscopy performed on the recycled carbon fibers showed no change in comparison to the virgin fibers (Figures 9D and 9E). To further prove that the recycled carbon fibers had not been damaged, a new composite was prepared using a new vitrimer resin. The flexural stress-strain curves (Figure S33) of the pristine vitrimer composite and the recycled vitrimer composite were almost the same, a proof that the recycling method not only allows for the recycling of the reinforcements but also preserves the fibers' structure and any their mechanical properties.

The exceptional properties of carbon fibers have driven a significant increase in their market demand over recent decades. However, recycling carbon-fiber-reinforced thermoset composites remains challenging because the matrix cannot be

CellPress
OPEN ACCESS

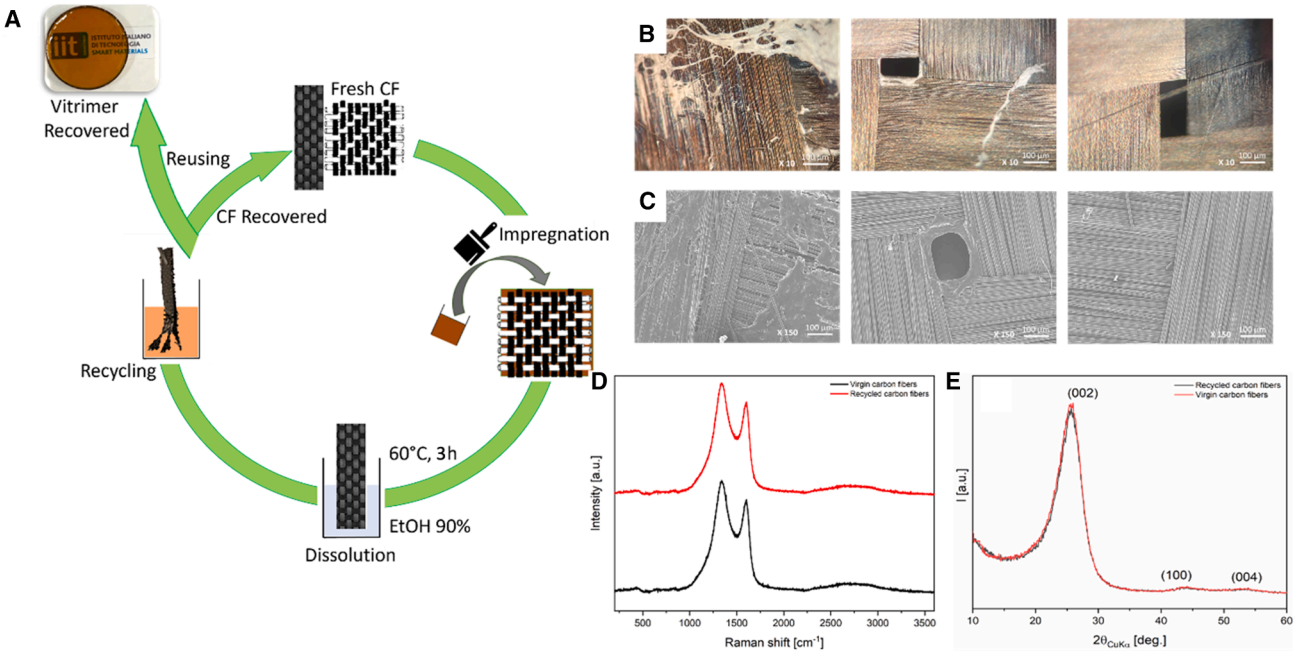


Figure 9. Recycling of the PHTE-vitrimer composite

(A) Recyclability scheme of the PHTE-vitrimer composite.

(B and C) Optical (B) and SEM (C) images of recycled carbon fibers at different times of the process: 0, 1.5, and 3 h.

(D) Raman spectra of the virgin and recycled carbon fibers.

(E) XRD patterns of the virgin and recycled carbon fibers.

removed without damaging the fibers. This limitation continues to be the primary barrier to the sustainable reuse of carbon fibers. The chemical recycling approach presented here overcomes this challenge by enabling the recovery of both the vitrimer matrix and the carbon fibers under mild conditions, thereby preserving fiber integrity and mechanical performance.

Furthermore, given the high cost of carbon fibers, recycling them without compromising their performance characteristics could yield substantial economic benefits.[58,59] This recycling method is also applicable to the EPP-based composite, allowing recovery of both the matrix and the carbon fibers (Figure S34). In contrast, the commercial epoxy thermoset did not dissolve in 90% v/v ethanol, preventing the recycling of the composite and recovery of the carbon (Figure S35; Table S8).

METHODS

Procedure for the hydrolysis of the 1,4-butanediol diglycidyl ether (BDGE hydrolyzed)

Desired amounts of 1,4-butanediol diglycidyl ether and water were placed in a glass flask at 95°C, and the resulting solution was stirred with a magnetic stirrer for 24 h. Subsequently, the water was removed under reduced pressure to obtain the target compound. The successful reaction was confirmed by the ^{1}H-NMR analysis (Figure S2).

Boronic ester cross-linker synthesis

1 equivalent of component A (molecule with two diols functionalization chosen among diglycerol, pentaerythritol, and BDGE hydrolyzed) and 2 equivalents of a component B (a boronic acid chosen from 2-aminophenyl boronic acid, 3-aminophenyl boronic acid, 3-hydroxybenzeneboronic acid, 3-carboxybenzeneboronic acid, and 3-mercaptobenzeneboronic acid) were placed in a glass flask with a magnetic stirrer at RT in EtOH (1 mol component B in 1,025 mL solvent) (Scheme 1). The resulting mixture became homogenous in about 5 min and was stirred for 24 h. Subsequently, the solvent was removed under reduced pressure to obtain the target compound without further purification (Figure 1). NMR, DSC data, and reaction scheme for each of the syntheses are reported in Figures S5, S6, S7, S8, S9, S10, S11, S1, and S13, and final conversion of the synthesis is reported in Table S3. ^{1}H-NMR spectra of the final mixture were composed primarily by the target products, unless specified.

Thiol functionalized cross-linker

m-MDGBE [3,3′-((oxybis(methylene))bis(1,3,2-dioxaborolane-4,2-diyl))dibenzenethiol, (diMercapto DiGlycerol diBoronic Ester, m-MDGBE)] was prepared starting from 3-thiolbenzene boronic acid and diglycerol and obtained with low purity as white solid with a melting point (T_m) of 53°C (Figure S5). The ^{1}H NMR spectra show a large number of by-products, thus the target product has been obtained with low purity.

Amino functionalized cross-linkers

m-DGBEA [3,3′-((oxybis(methylene))bis(1,3,2-dioxaborolane-4,2-diyl))dianiline, (meta-DiGlycerol diBoronic Ester diAmino, *m*-DGBEA)] synthetized from diglycerol, and 3-aminophenyl boronic acid was obtained as viscous liquid at RT with a T_g= 10°C, and it is thermally stable up to 250°C. NMR peak assignation is as follows: ^{1}H-NMR (400 MHz, $CDCl_3$), δ (ppm): 3.63–3.73 (m, 4H,

OCH_2); 4.09–4.17 (m, 2H, B-OCH_2); 4.33–4.38 (t, 2H, B-OCH_2, J = 8 Hz); 4.65–4.72 (m, 2H, B-OC*H*); 6.81–6.78 (m, 2H, C*H arom*); 7.19–7.10 (m, 6H, C*H arom*).

^{13}C-NMR (100 MHz, $CDCl_3$), δ (ppm): 63.7 (OCH_2 of longer polyglycerol chains); 68.2 (B-OCH_2); 73.7(OCH_2); 76.1 (B-OCH); 118.3; 121.3; 125.1; 128.9; 146.0.

o-DGBEA [2,2′-((oxybis(methylene))bis(1,3,2-dioxaborolane-4,2-diyl))dianiline, (orto-DiGlycerol diBoronic Ester diAmino, *o*-DGBEA)] were synthetized from diglycerol, and 2-aminophenyl boronic acid was obtained as viscous liquid but with scarce thermal stability, since it degrades below 35°C. NMR peak assignation is as follows: ^{1}H-NMR (400 MHz, $CDCl_3$), δ (ppm): 3.58–3.73 (m, 4H, OCH_2); 4.02–4.15 (m, 2H, B-OCH_2); 4.27–4.34 (t, 2H, B-OCH_2, J = 8 Hz); 4.55–4.65 (m, 2H, B-OC*H*); 6.48–6.54 (m, 2H, C*H* arom); 6.56–7.63 (m, 2H, C*H* arom); 7.02–7.20 (m, 2H, C*H* arom); 7.50–7.55 (m, 2H, C*H* arom).

^{13}C-NMR (100 MHz, $CDCl_3$), δ (ppm): 63.72 (OCH_2 of longer polyglycerol chains); 68.3 (B-OCH_2); 71.6 (OCH_2); 72.6 (B-OCH); 118.3; 121.3; 125.1; 128.8; 145.8.

m-BDBEA [3,3′-(((butane-1,4-diylbis(oxy))bis(methylene))-bis(1,3,2-dioxaborolane-4,2-diyl))dianiline, (meta-ButaneDiol diBoronic Ester diAmino, m-BDBEA)] was prepared starting from BDGE hydrolyzed and 3-amino phenyl boronic acid as viscous liquid at RT with T_g= 0°C. NMR peak assignation is as follows: ^{1}H-NMR (400 MHz, $CDCl_3$), δ (ppm): 1.54 (m, 4H, OCH_2CH_2); 3.26–3.51 (m, 8H, OCH_2); 4.02–4.10 (m, 2H, B-OCH_2); 4.26–4.32 (t, 2H, B-OCH_2, J = 8 Hz); 4.53–4.61 (m, 2H, B-OC*H*); 6.48–6.73 (m, 2H, C*H arom*); 7.04–7.19 (m, 6H, C*H arom*).

^{13}C-NMR (100 MHz, $CDCl_3$), δ (ppm): 63.7; 67.8; 73.5;73.6; 75.7; 114.9; 117.1; 133.1; 136.9; 153.7.

m-PTBEA [3,3′-(2,4,8,10-tetraoxa-3,9-diboraspiro[5.5]undecane-3,9-diyl)dianiline, (meta-Pentaertrhrytol diBoronic Ester diAmino, *m*-PTBEA)] prepared from pentaerythritol, and 3-aminophenyl boronic acid has been obtained as white solid at RT with no detectable T_m up to 150°C (from Figures S6, S7, S8, and S9). NMR peak assignation is as follows: ^{1}H-NMR (400 MHz, $CDCl_3$), δ (ppm): 3.97 (s, 8H, B-OCH_2); 6.70–6.73 (m, 2H, C*H arom.*); 7.04–7.15 (m, 6H, C*H arom.*).

^{13}C-NMR (100 MHz, DMSO-d_6), δ (ppm): 64.2 (B-OCH_2); 116.9; 119.9; 121.7; 128.5; 148.3.

Hydroxyl functionalized cross-linkers

m-HDGBE [3,3′-((oxybis(methylene))bis(1,3,2-dioxaborolane-4,2-diyl))diphenol, (diHydroxyl DiGlycerol diBoronic Ester, m-HDGBE)] was synthetized from 3-hydroxybenzene boronic acid and diglycerol, and it was obtained as viscous liquid at RT with a T_g= 9°C. NMR peak assignation is as follows: ^{1}H-NMR (400 MHz, $CDCl_3$), δ (ppm): 2.22 (br, 2H, OH); 3.51–3.67 (m, 4H, OCH_2); 3.97–4.07 (m, 2H, B-OCH_2); 4.19–4.27 (t, 2H, B-OCH_2, J = 8 Hz); 4.55–4.63 (m, 2H, B-OC*H*); 6.81–6.89 (m, 2H, C*H arom.*); 7.06–7.625 (m, 6H, C*H arom.*).

^{13}C-NMR (100 MHz, $CDCl_3$), δ (ppm): 67.7 (B-OCH_2); 73.1 (OCH_2); 76.1 (B-OC*H*); 119.0; 125.6; 129.6; 157.2.

m-HBDBE [3,3'-(((butane-1,4-diylbis(oxy))bis(methylene))-bis(1,3,2-dioxaborolane-4,2-diyl))diphenol, (diHydroxyl ButaneDiol diBoronic Ester, *m*-HBDBE)] was obtained as viscous liquid with a T_g= −9°C starting from BDGE hydrolyzed and 3-hydroxyphenyl boronic acid (Figures S10 and S11). NMR peak assignation is as follows: ^{1}H-NMR (400 MHz, $CDCl_3$), δ (ppm): 1.54 (m, 4H, OCH_2CH_2); 2.1 (br, 2H, O*H*); 3.60–3.70 (m, 4H, OCH_2); 3.99–4.12 (m, 2H, B-OCH_2); 4.26–4.34 (t, 2H, B-OCH_2, J = 8 Hz); 4.55–4.65 (m, 2H, B-OC*H*); 6.50 (s, 2H, C*H arom.*); 6.87–6.91 (m, 2H, C*H arom.*); 7.13–7.30 (m, 4H, C*H arom.*).

^{13}C-NMR (100 MHz, DMSO-d_6), δ (ppm): 26.2; 68.0; 71.0 (B-OCH2); 72.3 (OCH2); 76.3 (B-OCH); 119.0; 121.3; 125.6; 129.6; 157.3.

Carboxyl functionalized cross-linkers

m-CDGBE [3,3′-((oxybis(methylene))bis(1,3,2-dioxaborolane-4,2-diyl))dibenzoic acid, (diCarboxyl DiGlycerol diBoronic Ester, *m*-CDGBE)] was synthetized from 3-carboxybenzene boronic acid and diglycerol and was obtained as white solid with no T_m up to 150°C.

NMR peak assignation is as follows: ^{1}H-NMR (400 MHz, $CDCl_3$), δ (ppm): 3.61–3.78 (m, 4H, OCH_2); 4.11–4.17 (m, 2H, B-OCH_2); 4.29–4.35 (t, 2H, B-OCH_2, J = 8 Hz); 4.63–4.70 (m, 2H, B-OC*H*); 7.34–7.46 (m, 2H, C*H arom.*); 7.88–7.92 (d, 2H, C*H arom.*); 8.08–8.1 (d, 2H, C*H arom.*); 8.39 (s, 2H, C*H arom.*).

^{13}C-NMR (100 MHz, DMSO-d_6), δ (ppm): 68.1 (B-OCH_2); 73.1 (OCH_2); 77.3 (B-OCH); 129.1; 132.8; 135.9; 139.1; 167.7.

m-CBDBE [3,3′-(((butane-1,4-diylbis(oxy))bis(methylene))-bis(1,3,2-dioxaborolane-4,2-diyl))dibenzoic acid, (diCarboxyl ButaneDiol diBoronic Ester, m-HBDBE)] was obtained as solid, starting from BDGE hydrolyzed and 3-hydroxy phenyl boronic acid and presented no T_m up to 150°C (Figures S12 and S13).

NMR peak assignation is as follows: ^{1}H-NMR (400 MHz, $CDCl_3$), δ (ppm): 1.58 (s, 4H, CH_2); 3.40–3.68 (m, 8H, OCH_2); 4.06–4.11 (m, 2H, B-OCH_2); 4.32–4.38 (t, 2H, B-OCH_2, J = 8 Hz); 4.63–4.71 (m, 2H, B-OC*H*); 7.38–7.45 (m, 2H, C*H arom.*); 7.93–7.98 (d, 2H, C*H arom.*); 8.08–8.11 (d, 2H, C*H arom.*); 8.46–8.49 (m, 2H, C*H arom.*).

^{13}C-NMR (100 MHz, DMSO-d_6), δ (ppm): 26.12; 68.2 (B-OCH2); 71.1; 72.2 (OCH2); 76.6 (B-OCH); 128.6; 130.8; 132.6; 135.7; 139.1; 167.9.

Additionally, NMR spectra, DSC, data and reaction scheme for each of the syntheses are reported in Figures S5, S6, S7, S8, S9, S10, S11, S12, and S13, and final conversion of the syntheses are reported in Table S3.

p-DBEDT cross-linker has been prepared following the synthetic procedure described by Zych et al. and used as a comparative example.[10]

To demonstrate the feasibility of the synthesis in different solvents, meta-Diglycerol diboronic ester diamino (*m*-DGBEA) cross-linker synthesis was also performed in acetone, ethyl acetate, methyl tetrahydrofuran (2-Me THF), and anisole, and the resulting mixtures were analyzed by ^{1}H-NMR. (Figure S3).

Vitrimer synthesis

Vitrimers were synthetized by combining one of the above cross-linkers with an epoxy precursor, either PHTE (Phloroglucinol triglycidyl ether) or EPP (bisphenol A diglycidyl ether-based commercial pre-polymer, with an epoxide to nucleophile molar ratio of 1:1). The two components were mixed upon gentle heating in a Teflon mold and cured at RT for 24 h, following a post-curing treatment in the oven at 60°C for 3 h. Specifically, this curing

procedure was adopted to mimic the mild conditions used for standard commercial epoxy resins, maximizing operational compatibility and minimizing energy costs.

Procedure for commercial epoxy resin cross-linking (reference material)

Desired amount of EPP and commercial polyamine-based hardener (pre-polymer to hardener mass ratio of 2:1) was placed in a Teflon mold and mixed until the mixture became homogenous (around 2 min) and cured at RT for 24 h.[9]

Procedure for the fabrication of the composites

Carbon fiber-reinforced composites were prepared by overlapping and impregnating three carbon fiber layers with dimensions of 10 × 10 cm^2 with 30 g of the commercial epoxy resin or the vitrimer resin using a spatula. The impregnated layers were placed between two metal sheets with 9 kg weight on top to ensure adhesion between the fibers and the resin and to remove the excess resin. The composites were cured for 24 h at RT and, for the vitrimer resin, a post-curing at 60°C for 3 h was applied (Figure 8A).[9]

Measurements

Infrared spectra were obtained with a single-reflection attenuated total reflection (ATR) accessory (MIRacle ATR, PIKE Technologies) coupled to a Fourier Transform Infrared (FTIR) spectrometer (Brucker Vertex 70V). All spectra were recorded under vacuum in the 4,000–500 cm^{-1} range with a resolution of 4 cm^{-1}, accumulating 32 scans.

^1H NMR analysis was carried out at RT using 5 mm tubes on an Avance III 400 MHz spectrometer, Bruker. Each sample was weighed (about 5–10 mg) and dissolved in 500 μL deuterated solvent ($CDCl_3$ or DMSO-d_6). Chemical shifts are reported in ppm and were determined by reference to tetramethyl silane (TMS).

Gel fraction was determined by weighing a small piece (~200 mg) of a material and placing it in a vial with 10 mL of ethyl acetate for 24 h. Then, the ethyl acetate was removed, and the remaining undissolved part of the material was washed with ethyl acetate, dried under vacuum at 50°C for 24 h, and weighed again. Gel fraction was calculated according to the formula: Gel Fraction = [(mass of the dried sample after the test) / (mass of the sample before the test)] * 100.

Density of the vitrimers, commercial epoxy thermoset, and their carbon fiber composites were evaluated by cutting rectangular pieces for each sample, measuring all the dimensions and weighing them on an analytical balance to measure their mass, according to the formula: Density = (mass of the sample) / (volume of the sample).

Bending test was performed using a dual column Instron 3365 universal testing machine equipped with 2 KN load cell and a three-point bend fixture with a 10 mm anvil. Rectangular-shaped samples with 6 × 1 cm^2 dimensions and thickness of 1 mm were cut out directly from matrices and composites. The error bars shown in the corresponding graph indicate the standard deviation of the measurements

Reprocessability tests were performed by compression molding under 4 tons of pressure for 5 min at 100°C using Carver 3853 CE press. The obtained sheets were cut into rectangular pieces and underwent the bending test four times. After the first cycle, all the tested samples and the residual pieces of the vitrimers went through compression molding again and were cut again into rectangular-shaped samples and tested at the bending tester. At least five measurements were carried out for each sample, and the results were averaged to obtain a mean value. Flexural modulus values were calculated using the built-in software of the bending tester.

Chemical recyclability of the vitrimer was performed by dissolving around 200 mg of vitrimer and commercial epoxy in 90:10 v/v EtOH:water solution for 20 min at 60°C, while the dissolution lasted 3 h at 60°C for the composites. Subsequently, the solutions were cast, and ethanol was allowed to evaporate to regenerate the vitrimer.

Differential scanning calorimetry (DSC) was performed using Discovery DSC 250, TA Instruments. The analyses on the cross-linker were carried out at a heating and cooling rate of 10°C/min from −50°C to 150°C with nitrogen as cell purge gas (50 ml/min). The measurements on the vitrimers were carried out at a heating and cooling rate of 10 °C/min from 0°C to 200°C with nitrogen as cell purge gas (50 mL/min). Glass transition temperatures were obtained from the second heating curve.

Thermogravimetric analysis (TGA) was performed on TGA Q 500, TA Instruments analyzer under nitrogen atmosphere (flux: 50 ml/min) from 30°C to 800 °C at a heating rate of 10°C/min.

Optical microscopy images were taken with Leica DFC 420 optical microscFaope with a 10× magnification.

SEM analysis was conducted by JEOL JSM-6490LA scanning electron microscope (SEM), with an acceleration voltage of 10 kV with a 150× magnification, on samples coated with gold.

DMTA/stress relaxation was performed using a DMTA TA Q800 in temperature sweep mode. Samples were tested in temperature sweeps from −50°C to 100°C with a heating rate of 2°C min^{-1}. Experiments were performed in a single frequency oscillation mode with a frequency of 1 Hz and a displacement amplitude of 0.1% in auto tension offset control.

Rheology analyses were performed using an Ares rheometer, TA instruments. All measurements were carried out in plate-plate geometry (1 mm thickness). Frequency sweeps were carried out from 100 to 0.01 Hz from 80°C to 160°C with a constant strain amplitude of 1%.

Biodegradability was assessed by measuring the biochemical oxygen demand (BOD) with OxiTop-IDS system. The BOD was determined by monitoring the oxygen consumption in a closed bottle filled with 432 mL of seawater to mimic real environmental conditions, since it contains microorganisms and nutrients needed for their growth. Samples were tested in duplicates, and the experiments were conducted at RT inside dark glass bottles hermetically closed with the OxiTop measuring head. Sodium hydroxide was used as a CO_2 scavenger to sequestrate carbon dioxide produced during biodegradation, and biotic consumption of the oxygen present in the free volume of the system was measured as decrease in pressure. Raw data of oxygen consumption (mg O_2/L) were corrected by subtracting the mean values of the blanks, obtained by measuring the oxygen consumption of the seawater in the absence of any test material. After this subtraction, values were normalized on the mass of

the individual samples and referred to 100 mg of the material (mg O_2/100 mg). Cotton and poly-propylene were added as reference samples.[9] The ThOD was calculated from the elemental composition of the compound, following stoichiometric principles for complete oxidation of carbon, hydrogen, sulphur, and nitrogen to CO_2, H_2O, SO^{2-} and NO_3^-, respectively, according to the formula: theoretical oxygen demand = $\frac{\left(c+\frac{h}{4}-\frac{o}{2}+5\frac{n}{4}+s\right)*32}{MW_{substance}}$, according to ISO 14851. The biodegradation percentage was, instead, determined as the ratio between the measured BOD and the ThOD, according to the formula: biodegradation percentage = (BOD/ThOD) *100.

Chemicals and materials

1,4-phenyldiboronic acid (1,4-PBA) (97%), 2-aminophenyl boronic acid (o-ABA) (97%), 3-aminophenyl boronic acid (m-ABA) (95%), 3-carboxybenzeneboronic acid (m-CBA) (97%), 3-hydroxybenzeneboronic acid (m-HBA) (97%), and 3-mercaptobenzeneboronic acid (m-MBA) (98%) were purchased from FluoroChem. Diglycerol was kindly provided by Spiga Nord SPA (Italy), and its impurities were quantified through NMR analysis as glycerol (3%), triglycerol/polyglycerols (28%) (Figure S1). 2-methyltetrahydrofuran (2-Me THF), acetone, anisole, ethanol (EtOH, 96%), ethyl acetate (EtOAc), deuterated chloroform ($CDCl_3$) and deuterated dimethyl sulfoxide (DMSO-d_6), pentaerythritol, 1,4-butanediol diglycidyl ether (BDGE), and thioglycerol were purchased from Merck.

Phloroglucinol triglycidyl ether (PHTE) with an average molecular weight of 294.30 g/mol and average number of epoxy groups per molecule of 3 was purchased from Specific polymers (France). Bicomponent (epoxy pre-polymer EPP and amino hardener) C-Systems 10 10 CFS epoxy resin (commercial epoxy resin) was purchased from Cecchi, Italy. All materials were used as received unless otherwise stated.

RESOURCE AVAILABILITY

Lead contact

All queries about experimental procedures can be directed to the lead contact, Dr. Davide Sangaletti (davide.sangaletti@iit.it).

Materials availability

All relevant vendors and preparation procedures are included in the paper.

Data and code availability

All relevant data are included in the paper and its supplemental information. Any additional information required to reanalyze the data reported in this paper is available from the lead contact upon request.

This paper does not report original code.

ACKNOWLEDGMENTS

This work is part of the ''Technologies for Sustainability'' flagship program of IIT. We thank Lara Marini (Istituto Italiano di Tecnologia, Smart Materials) for the TGA and DSC analysis, Luca Ceseracciu (Istituto Italiano di Tecnologia, Materials Characterization) for help with DMA measurements, Sergio Marras (Istituto Italiano di Tecnologia, Materials Characterization) for XRD analysis, Riccardo Carzino (Istituto Italiano di Tecnologia, Materials Characterization) for Raman measurements, and Luca Goldoni (Istituto Italiano di Tecnologia, Materials Characterization) for help with NMR measurements.

AUTHOR CONTRIBUTIONS

The manuscript was written through contributions of all authors. All authors have given approval to the final version of the manuscript. D.S.: conceptualization, methodology, validation, investigation, data curation, writing – original draft, visualization, project administration. A.Z.: conceptualization, methodology, validation, investigation, data curation, writing – review & editing, visualization, supervision, project administration. M.N.: methodology, investigation, writing – review & editing, supervision. A.F.: methodology, validation, investigation. G.P.: writing – review & editing, supervision. A.A.: writing – review & editing, supervision, funding acquisition.

DECLARATION OF INTERESTS

The authors declare that they have filed patent applications related to the subject matter of this work (application numbers: IT102024000005092 and PCT/IB2025/052180).

SUPPLEMENTAL INFORMATION

Supplemental information can be found online at https://doi.org/10.1016/j.xcrp.2026.103262.

Received: July 31, 2025
Revised: February 12, 2026
Accepted: March 24, 2026
Published: April 22, 2026

REFERENCES

1. Zheng, J., Png, Z.M., Ng, S.H., Tham, G.X., Ye, E., Goh, S.S., Loh, X.J., and Li, Z. (2021). Vitrimers: Current research trends and their emerging applications. Mater. Today *51*, 586–625. https://doi.org/10.1016/j.mattod.2021.07.003.
2. Guerre, M., Taplan, C., Winne, J.M., and Du Prez, F.E. (2020). Vitrimers: directing chemical reactivity to control material properties. Chem. Sci. *11*, 4855–4870. https://doi.org/10.1039/D0SC01069C.
3. Montarnal, D., Capelot, M., Tournilhac, F., and Leibler, L. (2011). Silica-like malleable materials from permanent organic networks. Science *334*, 965–968. https://doi.org/10.1126/science.1212648.
4. Sharma, H., Rana, S., Singh, P., Hayashi, M., Binder, W.H., Rossegger, E., Kumar, A., and Schlögl, S. (2022). Self-healable fiber-reinforced vitrimer composites: overview and future prospects. RSC Adv. *12*, 32569–32582. https://doi.org/10.1039/D2RA05103F.
5. Duval, A., Benali, W., and Avérous, L. (2024). Turning lignin into a recyclable bioresource: transesterification vitrimers from lignins modified with ethylene carbonate. Green Chem. *26*, 8414–8427. https://doi.org/10.1039/D4GC00567H.
6. Kumar, A., and Connal, L.A. (2023). Biobased Transesterification Vitrimers. Macromol. Rapid Commun. *44*, 2200892. https://doi.org/10.1002/marc.202200892.
7. Roig, A., Agizza, M., Serra, À., and De la Flor, S. (2023). Disulfide vitrimeric materials based on cystamine and diepoxy eugenol as bio-based monomers. Eur. Polym. J. *194*, 112185. https://doi.org/10.1016/j.eurpolymj.2023.112185.
8. Tian, P.-X., Li, Y.-D., Weng, Y., Hu, Z., and Zeng, J.-B. (2023). Reprocessable, chemically recyclable, and flame-retardant biobased epoxy vitrimers. Eur. Polym. J. *193*, 112078. https://doi.org/10.1016/j.eurpolymj.2023.112078.
9. Sangaletti, D., Ceseracciu, L., Marini, L., Athanassiou, A., and Zych, A. (2023). Biobased boronic ester vitrimer resin from epoxidized linseed oil for recyclable carbon fiber composites. Resour. Conserv. Recycl. *198*, 107205. https://doi.org/10.1016/j.resconrec.2023.107205.
10. Zych, A., Tellers, J., Bertolacci, L., Ceseracciu, L., Marini, L., Mancini, G., and Athanassiou, A. (2021). Biobased, Biodegradable, Self-Healing

Boronic Ester Vitrimers from Epoxidized Soybean Oil Acrylate. ACS Appl. Polym. Mater. *3*, 1135–1144. https://doi.org/10.1021/acsapm.0c01335.

11. Mah, J.J.Q., Feng, H., Surat'man, N.E.B., Li, B., Wang, S., and Li, Z. (2024). Water-resistant boronic ester vitrimer with hydrophobic side chain protection. Chem. Commun. *60*, 14220–14223. https://doi.org/10.1039/D4CC04981K.
12. Nardi, M., Ceseracciu, L., Scribano, V., Contardi, M., Athanassiou, A., and Zych, A. (2024). Sustainable adhesives: Exploring boronic ester vitrimers containing lignin microparticles. Chem. Eng. J. *495*, 153400. https://doi.org/10.1016/j.cej.2024.153400.
13. Debsharma, T., Amfilochiou, V., Wróblewska, A.A., De Baere, I., Van Paepegem, W., and Du Prez, F.E. (2022). Fast Dynamic Siloxane Exchange Mechanism for Reshapable Vitrimer Composites. J. Am. Chem. Soc. *144*, 12280–12289. https://doi.org/10.1021/jacs.2c03518.
14. Islam, M.S., Kedziora, G., Lee, J., Stafford, A., Varshney, V., Nepal, D., Baldwin, L.A., and Roy, A.K. (2024). Efficiency and Mechanism of Catalytic Siloxane Exchange in Vitrimer Polymers: Modeling and Density Functional Theory Investigations. J. Phys. Chem. A *128*, 5627–5636. https://doi.org/10.1021/acs.jpca.4c01394.
15. Röttger, M., Domenech, T., van der Weegen, R., Breuillac, A., Nicolaÿ, R., and Leibler, L. (2017). High-performance vitrimers from commodity thermoplastics through dioxaborolane metathesis. Science *356*, 62–65. https://doi.org/10.1126/science.aah5281.
16. van Hurne, S., Kisters, M., and Smulders, M.M.J. (2023). Covalent adaptable networks using boronate linkages by incorporating TetraAzaADamantanes. Front. Chem. *11*, 1148629. https://doi.org/10.3389/fchem.2023.1148629.
17. Gosecki, M., and Gosecka, M. (2022). Boronic Acid Esters and Anhydrates as Dynamic Cross-Links in Vitrimers. Polymers *14*, 842. https://doi.org/10.3390/polym14040842.
18. Lei, Y., Zhang, A., and Lin, Y. (2020). Reprocessability of dynamic polydioxaborolane networks activated by heat, moisture and mechanical force. Polymer *209*, 123037. https://doi.org/10.1016/j.polymer.2020.123037.
19. Chen, Y., Tang, Z., Liu, Y., Wu, S., and Guo, B. (2019). Mechanically Robust, Self-Healable, and Reprocessable Elastomers Enabled by Dynamic Dual Cross-Links. Macromolecules *52*, 3805–3812. https://doi.org/10.1021/acs.macromol.9b00419.
20. Breuillac, A., Kassalias, A., and Nicolaÿ, R. (2019). Polybutadiene Vitrimers Based on Dioxaborolane Chemistry and Dual Networks with Static and Dynamic Cross-links. Macromolecules *52*, 7102–7113. https://doi.org/10.1021/acs.macromol.9b01288.
21. Shi, Y., Hong, Y., Hong, J., Yu, A., Lee, M.W., Lee, J., and Goh, M. (2022). Bio-based boronic ester vitrimer for realizing sustainable and highly thermally conducting nanocomposites. Compos. B Eng. *244*, 110181. https://doi.org/10.1016/j.compositesb.2022.110181.
22. Demchuk, Z., Zhao, X., Shen, Z., Zhao, S., Sokolov, A.P., and Cao, P.-F. (2024). Tuning the Mechanical and Dynamic Properties of Elastic Vitrimers by Tailoring the Substituents of Boronic Ester. ACS Mater. Au *4*, 185–194. https://doi.org/10.1021/acsmaterialsau.3c00074.
23. Ma, Y., Liu, H., Wu, J., Yuan, L., Wang, Y., Du, X., Wang, R., Marwa, P.W., Petlulu, P., Chen, X., and Zhang, H. (2019). The adverse health effects of bisphenol A and related toxicity mechanisms. Environ. Res. *176*, 108575. https://doi.org/10.1016/j.envres.2019.108575.
24. Auvergne, R., Caillol, S., David, G., Boutevin, B., and Pascault, J.P. (2014). Biobased thermosetting epoxy: present and future. Chem. Rev. *114*, 1082–1115. https://doi.org/10.1021/cr3001274.
25. Krishnakumar, B., Pucci, A., Wadgaonkar, P.P., Kumar, I., Binder, W.H., and Rana, S. (2022). Vitrimers based on bio-derived chemicals: Overview and future prospects. Chem. Eng. J. *433*, 133261. https://doi.org/10.1016/j.cej.2021.133261.
26. Chong, K.L., Lai, J.C., Rahman, R.A., Adrus, N., Al-Saffar, Z.H., Hassan, A., Lim, T.H., and Wahit, M.U. (2022). A review on recent approaches to sustainable bio-based epoxy vitrimer from epoxidized vegetable oils. Ind. Crop. Prod. *189*, 115857. https://doi.org/10.1016/j.indcrop.2022.115857.
27. Sahoo, S.K., Mohanty, S., and Nayak, S.K. (2015). Toughened bio-based epoxy blend network modified with transesterified epoxidized soybean oil: synthesis and characterization. RSC Adv. *5*, 13674–13691. https://doi.org/10.1039/C4RA11965G.
28. Łukaszczyk, J., Janicki, B., and Kaczmarek, M. (2011). Synthesis and properties of isosorbide based epoxy resin. Eur. Polym. J. *47*, 1601–1606. https://doi.org/10.1016/j.eurpolymj.2011.05.009.
29. Ma, Z., Wang, Y., Zhu, J., Yu, J., and Hu, Z. (2017). Bio-based epoxy vitrimers: Reprocessibility, controllable shape memory, and degradability. J. Polym. Sci., Part A: Polym. Chem. *55*, 1790–1799. https://doi.org/10.1002/pola.28544.
30. Turi, E.A. (1981). Thermal Characterization of Polymeric Materials (Academic Press).
31. Xue, B., Tang, R., Xue, D., Guan, Y., Sun, Y., Zhao, W., Tan, J., and Li, X. (2021). Sustainable alternative for bisphenol A epoxy resin high-performance and recyclable lignin-based epoxy vitrimers. Ind. Crop. Prod. *168*, 113583. https://doi.org/10.1016/j.indcrop.2021.113583.
32. Zhao, S., and Abu-Omar, M.M. (2016). Renewable Epoxy Networks Derived from Lignin-Based Monomers: Effect of Cross-Linking Density. ACS Sustain. Chem. Eng. *4*, 6082–6089. https://doi.org/10.1021/acssuschemeng.6b01446.
33. Achkar, J., Xian, M., Zhao, H., and Frost, J.W. (2005). Biosynthesis of Phloroglucinol. J. Am. Chem. Soc. *127*, 5332–5333. https://doi.org/10.1021/ja042340g.
34. Noè, C., Malburet, S., Bouvet-Marchand, A., Graillot, A., Loubat, C., and Sangermano, M. (2019). Cationic photopolymerization of bio-renewable epoxidized monomers. Prog. Org. Coating *133*, 131–138. https://doi.org/10.1016/j.porgcoat.2019.03.054.
35. Okada, Y., Ishimaru, A., Suzuki, R., and Okuyama, T. (2004). A new phloroglucinol derivative from the brown alga Eisenia bicyclis: potential for the effective treatment of diabetic complications. J. Nat. Prod. *67*, 103–105. https://doi.org/10.1021/np030323j.
36. United Nations. The 17 goals. https://sdgs.un.org/goals.
37. Tran, H.T.T., Nisha, S.S., Radjef, R., Nikzad, M., Bjekovic, R., and Fox, B. (2024). Recyclable and Biobased Vitrimers for Carbon Fibre-Reinforced Composites—A Review. Polymers *16*, 1025.
38. Sharma, H., Kumar, A., Rana, S., Sahoo, N.G., Jamil, M., Kumar, R., Sharma, S., Li, C., Kumar, A., Eldin, S.M., and Abbas, M. (2023). Critical review on advancements on the fiber-reinforced composites: Role of fiber/matrix modification on the performance of the fibrous composites. J. Mater. Res. Technol. *26*, 2975–3002. https://doi.org/10.1016/j.jmrt.2023.08.036.
39. Fiber Reinforced Polymer (FRP) Composites Market. https://www.grandviewresearch.com/industry-analysis/fiber-reinforced-polymer-frp-composites-market.
40. Lamm, M.E., Li, P., Hankinson, S., Zhu, T., and Tang, C. (2019). Plant oil-derived copolymers with remarkable post-polymerization induced mechanical enhancement for high performance coating applications. Polymer *174*, 170–177. https://doi.org/10.1016/j.polymer.2019.04.072.
41. https://www.knowledge-sourcing.com/report/carbon-fiber-reinforced-thermoplastic-cfrtp-composite-market.
42. Goodman, S.H. (1998). 1 - Introduction. In Handbook of Thermoset Plastics, Second Edition, S.H. Goodman, ed. (William Andrew Publishing), pp. 1–22. https://doi.org/10.1016/B978-081551421-3.50004-7.
43. Goodman, S.H. (1998). 6 - Epoxy Resins. In Handbook of Thermoset Plastics, Second Edition, S.H. Goodman, ed. (William Andrew Publishing), pp. 193–268. https://doi.org/10.1016/B978-081551421-3.50009-6.
44. Gusakova, K., Saiter, J.-M., Grigoryeva, O., Gouanve, F., Fainleib, A., Starostenko, O., and Grande, D. (2015). Annealing behavior and thermal stability of nanoporous polymer films based on high-performance Cyanate

Ester Resins. Polym. Degrad. Stabil. *120*, 402–409. https://doi.org/10.1016/j.polymdegradstab.2015.07.009.

45. Tang, S.K., Davey, R.J., Sacchi, P., and Cruz-Cabeza, A.J. (2020). Can molecular flexibility control crystallization? The case of para substituted benzoic acids. Chem. Sci. *12*, 993–1000. https://doi.org/10.1039/D0SC05424K.
46. Fox, T.G., and Loshaek, S. (1955). Influence of molecular weight and degree of crosslinking on the specific volume and glass temperature of polymers. J. Polym. Sci. *15*, 371–390. https://doi.org/10.1002/pol.1955.120158006.
47. Fox, T.G., Jr., and Flory, P.J. (1950). Second-Order Transition Temperatures and Related Properties of Polystyrene. I. Influence of Molecular Weight. J. Appl. Phys. *21*, 581–591. https://doi.org/10.1063/1.1699711.
48. Debenedetti, P.G., and Stillinger, F.H. (2001). Supercooled liquids and the glass transition. Nature *410*, 259–267. https://doi.org/10.1038/35065704.
49. Meng, F., Saed, M.O., and Terentjev, E.M. (2022). Rheology of vitrimers. Nat. Commun. *13*, 5753. https://doi.org/10.1038/s41467-022-33321-w.
50. Telatin, T., De la Flor, S., Montané, X., and Serra, À. (2024). Chemically Degradable Vitrimers Based on Divanillin Imine Diepoxy Monomer and Aliphatic Diamines for Enhanced Carbon Fiber Composite Applications. Polymers *16*, 2754.
51. Zych, A., Pinalli, R., Soliman, M., Vachon, J., and Dalcanale, E. (2020). Polyethylene vitrimers via silyl ether exchange reaction. Polymer *199*, 122567. https://doi.org/10.1016/j.polymer.2020.122567.
52. Zhao, Y., Qin, T., Jiang, C., Li, J., Xiong, Y., Liu, S., Qin, J., Shi, X., and Zhang, G. (2023). Boronic ester-based vitrimeric methylvinyl silicone elastomer with ''solid-liquid'' feature and rate-dependent mechanical performance. Polymer *265*, 125545. https://doi.org/10.1016/j.polymer.2022.125545.
53. Nishimura, Y., Chung, J., Muradyan, H., and Guan, Z. (2017). Silyl Ether as a Robust and Thermally Stable Dynamic Covalent Motif for Malleable Polymer Design. J. Am. Chem. Soc. *139*, 14881–14884. https://doi.org/10.1021/jacs.7b08826.
54. Denissen, W., Winne, J.M., and Du Prez, F.E. (2016). Vitrimers: permanent organic networks with glass-like fluidity. Chem. Sci. *7*, 30–38. https://doi.org/10.1039/c5sc02223a.
55. Wu, X., Huang, W., Zhao, Y., Ding, Z., Tang, C., and Zhang, J. (2013). Mechanisms of the Shape Memory Effect in Polymeric Materials. Polymers *5*, 1169–1202. https://doi.org/10.3390/polym5041169.
56. Cash, J.J., Kubo, T., Bapat, A.P., and Sumerlin, B.S. (2015). Room-Temperature Self-Healing Polymers Based on Dynamic-Covalent Boronic Esters. Macromolecules *48*, 2098–2106. https://doi.org/10.1021/acs.macromol.5b00210.
57. Kim, C., Ejima, H., and Yoshie, N. (2017). Non-swellable self-healing polymer with long-term stability under seawater. RSC Adv. *7*, 19288–19295. https://doi.org/10.1039/c7ra01778b.
58. Yu, K., Taynton, P., Zhang, W., Dunn, M.L., and Qi, H.J. (2014). Influence of stoichiometry on the glass transition and bond exchange reactions in epoxy thermoset polymers. RSC Adv. *4*, 48682–48690. https://doi.org/10.1039/C4RA06543C.
59. Isa, A., Nosbi, N., Che Ismail, M., Md Akil, H., Wan Ali, W.F.F., and Omar, M.F. (2022). A Review on Recycling of Carbon Fibres: Methods to Reinforce and Expected Fibre Composite Degradations. Materials *15*, 4991. https://doi.org/10.3390/ma15144991.